TECHNISCHE UNIVERSITÄT WIEN Vienna | Austria

Dissertation

Mixed kinematic modelling and simulation of slack belt drives using structural theories of rods and shells

carried out for the purpose of obtaining the degree of Doctor technicae (Dr. techn.), submitted at TU Wien, Faculty of Mechanical and Industrial Engineering

Jakob SCHEIDL

Mat. Nr.: 01127380

under the supervision of

Senior Scientist Mag. Dr. habil. Yury Vetyukov
Institute of Mechanics and Mechatronics, E325

Vienna, July 2021

reviewed by

Univ.Prof. Dipl.-Ing. Dr.techn. Michael Krommer
JKU Linz, Institute of Technical Mechanics (tmech)
Science Park 1, 4040 Linz, Austria

Associate Prof. Dipl.-Ing. Dr.techn. Heinz Pettermann
TU Wien, Institute of Lightweight Design and Structural Biomechanics (ILSB)
Getreidemarkt 9, 1060 Wien, Austria

This work was supported by the Austrian Research Promotion Agency (FFG) within the framework of the project *LaLaBand*, grant number 861493.

I confirm, that going to press of this thesis needs the confirmation of the examination committee.

Affidavit

I declare in lieu of oath, that I wrote this thesis and performed the associated research myself, using only literature cited in this volume. I confirm that this work is original and has not been submitted elsewhere for any examination, nor is it currently under consideration for a thesis elsewhere. I acknowledge that the submitted work will be checked using suitable and state-of-the-art means (plagiarism detection software).

City, date	Signature

Danksagung

Ich möchte mich herzlich bei den Mitarbeitern und Mitarbeiterinnen des Instituts für Mechanik und Mechatronik der TU Wien, insbesondere bei den Kollegen des Forschungsbereichs für Mechanik fester Körper, für die gute Zusammenarbeit und die amikale Atmosphäre bedanken.

Ein besonderer Dank gilt dem Betreuer meiner Dissertation, Dr. Yury Vetyukov, für seinen aufrichtigen wissenschaftlichen Stil, sein enormes persönliches Engagement und die kompetente Unterstützung in Forschungsfragen und bei der Arbeit an Veröffentlichungen.

Für die reibungslose Zusammenarbeit im Rahmen des FFG Projekts *LaLaBand*, das geteilte wissenschaftliche Interesse und den Mut zur Veröffentlichung der erzielten Ergebnisse in anerkannten Zeitschriften, danke ich dem Projektmanager Dr. Klemens Schulmeister und den beteiligten Mitarbeitern der Berndorf Band GmbH sehr herzlich.

Für ihre bedingungslose Unterstützung in allen Lebenslagen bin ich meinen engsten Familienmitgliedern zutiefst dankbar.

Contents

Abstract

The cumulative thesis is concerned with the development of numerical simulation models for slack belt drives. For this sake, classic Lagrangian finite elements are inefficient as they require uniform meshes or frequent re-meshing. Additionally, they are prone to produce spurious numeric oscillations because of the ever recurring motion of nodal points across the contact zone boundaries. The mixed Eulerian–Lagrangian (MEL) kinematic description overcomes these deficiencies by means of a transformation that replaces the axial material coordinate with a spatial one, which is aligned with the primary direction of axial motion.

In continuation of previous research, we apply the MEL approach for the first time to the benchmark problem of a two-pulley belt drive. The introduction of a problem-specific compound coordinate system with a looped spatial coordinate allows to decouple the gross axial motion of material particles in circumferential direction from the transverse deflections of the belt. Finite elements based on this novel description reside at fixed points of the looped Eulerian coordinate, while material is transported through the mesh in axial direction.

We consider planar string and rod models of the belt and verify the finite element simulations against semi-analytic reference solutions, as obtained through numerical integration of the corresponding boundary value problems. A spatial parametrisation of the primary fields facilitates the deduction of the governing system of ordinary differential equations, which is later restated in a form accessible to standard purpose solvers. We seek slack static configurations of the belt in frictionless contact with the pulleys, simulate the quasistatic transient run up or compute the steady-state motion. In regard to the latter, a novel iterative concept is developed that avoids the time consuming simulation of the transient motion and enables a direct solution of the stationary problem in the finite element framework. The assumed Coulomb dry friction law amounts to a belt creep theory type of solution in the contact domains. In general, the iterative augmented Lagrangian multiplier method is the preferred strategy to enforce the contact constraints in the finite element schemes, but it fails in certain cases owing to the particularities of the contact response of the employed structural theories; then, the inherently simpler penalty regularisation method is used instead.

In the framework of the industrial cooperation project *LaLaBand*, funded by the Austrian Research Promotion Agency, grant number 861493, we develop a shell finite element model in MEL kinematic description for the simulation of the phenomenon of lateral run-off in a slack steel belt drive with account for the geometric imperfections of the belt as well as the tilting motion of the steering drum. Coulomb dry friction is replaced with an elastic contact model for simplicity and increased robustness of the scheme. The construction of consistent finite element approximations in the MEL formulation for the shell requires the introduction of various extended shape functions to satisfy the C^1 continuity condition. The successful validation of the shell finite element model against a series of physical experiments concludes the application oriented part of the research.

Kurzfassung

Die vorliegende kumulative Dissertation befasst sich mit der Entwicklung strukturmechanischer Simulationsmodelle für schwach gespannte Riemen- und Bandtriebe, für die sich die übliche Lagrange'sche kinematische Beschreibung als ineffizient erweist. Im Kontext der Methode der finiten Elemente erzwingt die strikte Bindung von Knoten und materiellen Punkten eine Mitführung der Knotenpunkte in Umfangsrichtung. Dieser axiale Transport ist ineffizient, weil er ein feines Diskretisierungsniveau für das gesamte Modell erfordert (für einen Umlauf durchläuft jeder Punkt die Kontaktzonen), und zudem einen stark veränderlichen Zeitverlauf der mitbewegten Zustandsgrößen bewirkt, der von numerischen Störungen zufolge des Ein- und Austritts von Knotenpunkten in den Kontaktbereich überlagert ist.

Die ursprünglich für axial bewegte Strukturen mit einfacher Geometrie eingeführte Euler–Lagrange'sche Beschreibung (engl. Abk. MEL für „mixed Eulerian–Lagrangian") hat diese Nachteile nicht. Sie beruht auf einer gemischten Parametrisierung des Lagevektors mithilfe einer in Hauptbewegungsrichtung der Struktur ausgerichteten räumlichen Koordinate und einer der Dimension des Raumes entsprechenden Anzahl von materiellen Koordinaten, die die Deformationen in transversaler Richtung erfassen. Dieser Koordinatenwechsel erlaubt die Konstruktion problemspezifischer finite Elemente Modelle mit in Fortbewegungsrichtung fixierten Elementen, die vom Material durchflossen werden.

Im Rahmen der Dissertation wird die MEL kinematische Beschreibung weiterentwickelt und erstmalig für schwach gespannte Riemen- und Bandtriebe adaptiert. Um die axiale Bewegung in der Hauptrichtung von den Deformationen in transversaler Richtung zu trennen, wird eine geschlossene, der Geometrie des Riementriebes angepasste, räumliche Koordinate eingeführt. Es werden verschiedene finite Elemente Modelle auf Basis klassischer strukturmechanischer Theorien für Seile und Balken zur Lösung folgender Problemstellungen entworfen: der statisch auf den Scheiben hängende Riemen, das quasistatische (langsame) Anlaufen und die stationäre (eingelaufene) Bewegung. Letztere kann mithilfe eines neu entwickelten Lösungskonzepts für finite Elemente direkt bestimmt werden, d.h. ohne zeitintensive Simulation der transienten Phase. Die iterative Methode der erweiterten Lagrange Multiplizierer zur Modellierung der Coulomb'schen Reibung scheitert zum Teil an numerischen Schwierigkeiten im Zusammenhang mit dem speziellen Verhalten klassischer Balkentheorien in Kontaktproblemen; in solchen Fällen wird auf die einfachere Strategie mit Straftermen (Penalty) zurückgegriffen.

Semi-analytische Vergleichslösungen durch numerische Integration der entsprechenden Randwertprobleme werden zur Validierung der Simulationsergebnisse herangezogen und tragen, insbesondere im Hinblick auf die Besonderheiten im Kontaktbereich, zu einem tieferen Verständnis der Mechanik bei. Der explizit vollzogene Koordinatenwechsel von der materiellen zu einer räumlichen Koordinate betont den Unterschied zwischen den beiden Perspektiven und erlaubt eine zeitinvariante Darstellung des stationären Problems als System gewöhnlicher Differentialgleichungen.

Im Rahmen des von der Österreichischen Forschungsförderungsgesellschaft FFG finanzierten Industrieprojektes *LaLaBand*, Identifikationsnummer 861493, wird ein Schalen

finite Elemente Modell zur Simulation des lateralen Laufverhaltens von schwach gespannten Prozesstahlbändern entwickelt. Geometrische Imperfektionen des Stahlbandes führen im Betrieb zum lateralen Verlaufen auf den Trommeln, d.h. zu einem Ablaufen in Richtung der Trommelachsen. Das mittels Experimenten am Teststand validierte Simulationsprogramm erlaubt eine Identifikation der kritischen Imperfektionen und trägt zur Entwicklung verbesserter Regelsysteme bei.

List of Figures

List of Tables

1. Introduction and scientific context

The function of countless mechanical systems such as bicycles, band-saws, cable-cars, audio-cassettes or conveyor systems to name but a few, relies on the operation of axially moving structures like: chains, cables, tapes or belts. Owing to this richness of different applications and the long standing tradition of research on axially moving structures, the available literature on this topic is rather extensive: from classic contributions concerned with transmission belt drives in the framework of Reynold's belt creep theory [1, 2] or Firbank's shear-theory for rubber belts with tensile cords [3], vibration studies on band-saw blades [4] or stability of moving beams [5], to research on Schallamach detachment waves in drives with high friction coefficient [6] and simulations of metal forming processes [7, 8], reeling analyses of composite oil pipes [9, 10] or the tailhook-catching of a plane on an aircraft carrier with an arresting cable system [11].

The contribution of the cumulative thesis to this lively field of research amounts to the further development of the *mixed Eulerian–Lagrangian* (MEL) kinematic description and its first application to slack belt drives utilizing a unified approach based on classic structural theories of rods or shells. In continuation of our past research on axially moving structures, which comprises the establishment of the MEL kinematic formulation [12, 13], its first applications to idealised belt drive systems [14, 15] and metal forming processes [8] as well as the study of dynamic oscillations of axially transported planar rods and strings [16], we implement the MEL kinematic formulation for the first time in a compound coordinate system that follows the geometric contour of the considered benchmark problem in a natural way and, thus, allows for an easy parametrisation of large transverse deflections. At heart, the MEL kinematic description rests upon a coordinate transformation from the axial material (Lagrangian) coordinate s to a spatial (Eulerian) coordinate σ; the parametrisation of a point in space is then truly mixed and given by the Eulerian variable σ and a corresponding number of material coordinates to account for deflections in transverse direction of the spatial contour.

In regard to finite element modelling for axially moving structures, the MEL approach allows for the transport of material across element boundaries in the primary direction of axial motion. In contrast, the nodal points of an element in classic Lagrangian description are obliged to move with the material particles. This entrained motion is particularly inefficient for the simulation of slack belt drives with large span width, as it requires a uniformly fine discretisation to ensure a sufficient resolution of the belt-to-drum contact at all times (each element passes through the contact domains in the course of a single revolution of the drive). Moreover, the continuous transport of nodal points across the contact zone boundaries induces spurious numerical oscillations with a mesh-size dependent frequency. The change of variable introduced in the MEL approach resolves this issue and facilitates spatially refined meshes, which increases computational efficiency; see [15] for a comparison of the different approaches in the example problem of an idealised belt drive.

The MEL formulation falls into the category of the well-known *Arbitrary Lagrangian Eulerian* (ALE) approaches. Contrary to traditional forms of ALE, which feature complicated mapping procedures between different parametrisations of the mechanical system [17, 18], the MEL strategy seeks a direct solution in the mixed coordinate space. Furthermore, the problem-specific parametrisation with a fixed Eulerian coordinate contributes to the convergence of simple time-integration routines and avoids the definition of a redundant set of unknowns, as opposed to modern ALE formulations related to flexible multibody dynamics [19, 20].

Several articles, which comprise the present thesis, are concerned with different kinds of rod models. In these papers we assume a Coulomb type of frictional contact to govern the belt-to-pulley interaction. In general, we refer to [21] for a review of established contact models and to [22] concerning the implementation in the finite element context. Here, we pursue an augmented Lagrangian strategy following the return-mapping algorithm originally proposed in [23], but employ the inherently simpler penalty regularisation approach in case the augmented procedure fails due to certain numerical difficulties, to be discussed in Sect. 6.3. Whenever feasible, semi-analytic solutions via numerical integration of the governing boundary value problem are computed to verify the corresponding finite element simulations and to provide a profound understanding for the behaviour of the classic structural theories; special attention is paid to the contact response in the presence of Coulomb dry friction. The primary distinctive features of the studies in the framework of planar rod theory in comparison to the ones available in the literature regarding analytical strategies, see [24, 25], as well as finite element modelling, see [26, 27], are:

- the MEL kinematic description in a compound coordinate system
- the focus on slack configurations with account for large transverse deflections in the field of gravity
- the rigorous unified approach to model the looped belt as a continuous structure
- the compound spatial parametrisation of variables in the boundary value problems, which accentuates the differences between the descriptions with spatial, hybrid and material coordinates

Beyond that, we develop a three-dimensional shell finite element model, see *Paper E*, to simulate the lateral run-off of a slack steel-conveyor belt in the framework of the industrial cooperation project *LaLaBand*, funded by the Austrian Research Promotion Agency (FFG), grant number 861493. This advanced formulation accounts for misaligned drum axes and geometric imperfections of the belt, which are introduced as intrinsic strains in the reference configuration, see [28, 29], employs a simplified elastic contact model in resemblance of belt-shear theory, see [30, 31], and requires extended shape functions to fulfil the C^1 continuity condition in the MEL kinematic description, see Sect. 7.2. It combines these features in an application-oriented scheme that allows for a justifiably accurate simulation of the lateral run-off in the – owing to the extreme membrane stiffness of a thin steel structure – adverse parameter range of a steel conveyor belt.

2. Problem statement and research goals

The work comprising this cumulative thesis continues the research and development of the mixed Eulerian–Lagrangian kinematic (MEL) approach, originally proposed to surmount the inherent deficiencies encountered when relying on the classic material (Lagrangian) description for the simulation of axially moving structures. In particular, it aims for an implementation of the MEL description in the benchmark problem of a slack two-pulley belt drive, depicted in Fig. 1. Corresponding finite element formulations and, if feasible, analytic strategies are developed following a unified approach based on different structural theories for the looped belt.

Simulation results obtained for planar rod problems of varying complexity are insightful regarding the general mechanics of slack belt drives and yet simple enough to be verified by means of semi-analytic reference solutions. This provides a solid basis for the development of an advanced shell finite element scheme aimed at the simulation of the lateral run-off of a steel belt drive with account for geometric imperfections and misaligned drum axes in the framework of the industrial research project *LaLaBand*.

To outline the methodical foundation of the thesis, we shall address the structural theories in the usual material (Lagrangian) description in Sect. 3 and Sect. 4, proceed with the MEL kinematic formulation for the belt drive problem in Sect. 5, explain the numerical treatment of frictional contact in Sect. 6, and conclude with a discussion of some finite element related aspects in Sect. 7. The five refereed contributions, which comprise the thesis (four journal publications and one book chapter) are shortly discussed in Sect. 8, where also the contribution of the author of the dissertation is presented in brief.

3. Geometrically nonlinear theory of rods in plane

We consider a planar rod as a one-dimensional continuum of material particles that is parametrised with the material arc coordinate $s \in [0,\, L]$ and placed in the xy-plane with Cartesian basis $\{\boldsymbol{i},\, \boldsymbol{j}\}$ and normal direction $\boldsymbol{k} = \boldsymbol{i} \times \boldsymbol{j}$. With the out-of-plane motion being constrained, we formally assign three degrees of freedom (two translations and one rotation) to each material particle. For the derivations ahead, we employ the following conventions: Greek indices take the values $\alpha = \{1, 2\}$, Einstein's summation convention applies to repeated indices, a prime denotes derivatives with respect to s and a dot corresponds to a total time derivative.

In the tradition of the director formulation for structural theories, see [32–34], we picture the deformation of a single material particle as a shift of its position from the undeformed reference state $\mathring{\boldsymbol{r}}$ to the actual one $\boldsymbol{r}$ further accompanied by a co-rotating, orthogonal basis $\boldsymbol{e}_\alpha$. The out-of plane direction remains $\boldsymbol{k} = \boldsymbol{e}_1 \times \boldsymbol{e}_2$ and an angle θ is introduced to relate the actual basis to the reference one:

$$\boldsymbol{e}_1 = \mathring{\boldsymbol{e}}_1 \cos\theta + \mathring{\boldsymbol{e}}_2 \sin\theta, \quad \boldsymbol{e}_2 = -\mathring{\boldsymbol{e}}_1 \sin\theta + \mathring{\boldsymbol{e}}_2 \cos\theta. \tag{1}$$

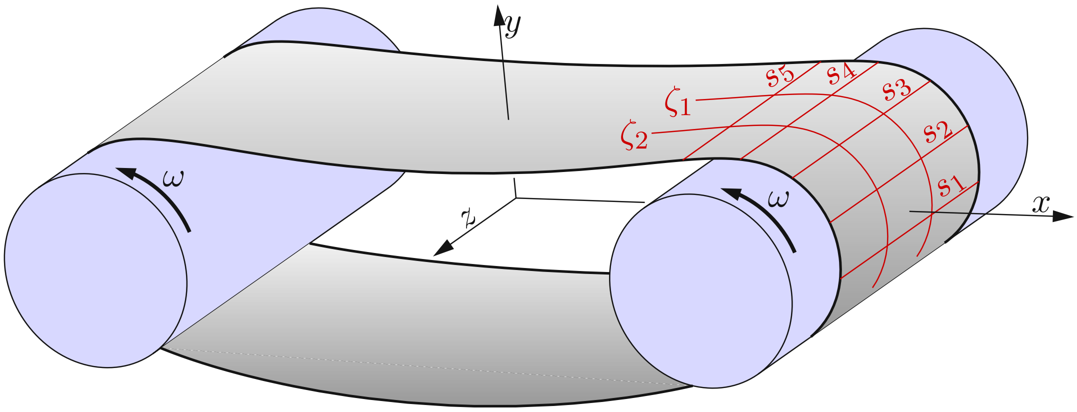

Figure 1: Model of a simple belt drive featuring a slack looped belt and two cylindrical drums operating at constant speed ω.

For the derivations ahead, it is efficient to define a rotation tensor $\mathbf{P}$:

$$\mathbf{P} = \boldsymbol{e}_\alpha \mathring{\boldsymbol{e}}_\alpha + \boldsymbol{k}\boldsymbol{k}, \quad \boldsymbol{e}_\alpha = \mathbf{P} \cdot \mathring{\boldsymbol{e}}_\alpha \tag{2}$$

to take care of the finite rotations of the material basis; the extension with the dyadic product of the out-of-plane direction $\boldsymbol{k}$ ensures regularity. We make use of the notion of dedicated vectors, to state the derivative and the variation of the rotation tensor:

$$\mathbf{P}' = \theta' \, \boldsymbol{k} \times \mathbf{P}, \quad \delta\mathbf{P} = \delta\theta \, \boldsymbol{k} \times \mathbf{P}. \tag{3}$$

In the framework of the direct approach [35], the principle of virtual work for a segment of the rod $s_0 \leq s \leq s_1$ is determined by the particular choice of particle degrees of freedom:

$$\int_{s_0}^{s_1} \left[\left(\boldsymbol{q} - \rho \, \ddot{\boldsymbol{r}} \right) \cdot \delta\boldsymbol{r} + \left(m - I \, \ddot{\theta} \right) \delta\theta - \delta\tilde{U} \right] \mathrm{d}s + \left[\boldsymbol{Q} \cdot \delta\boldsymbol{r} + M \, \delta\theta \right] \Big|_{s_0}^{s_1} = 0, \tag{4}$$

which features the virtual displacements $\delta\boldsymbol{r}$ and rotations $\delta\theta$. The virtual work of internal forces equals the negative variation of an elastic potential $\tilde{U}$. The distributed external forces $\boldsymbol{q}$ and moments m pair up with the corresponding inertia terms that feature the mass per unit reference length ρ and the moment of inertia I, respectively. The planar force $\boldsymbol{Q}(s)$ and bending moment $M(s)$ act on the boundaries of the considered segment from the adjacent parts of the rod ($s < s_0$ on the left, $s > s_1$ on the right). After incorporation of the boundary terms under the integral by means of partial integration, we argue that the integrand itself must vanish owing to the arbitrariness of variations:

$$\left(\boldsymbol{Q}' + \boldsymbol{q} - \rho \, \ddot{\boldsymbol{r}} \right) \cdot \delta\boldsymbol{r} + \left(M' + m - I \, \ddot{\theta} \right) \delta\theta - \delta\tilde{U} + M \, \delta\theta' + \boldsymbol{Q} \cdot \delta\boldsymbol{r}' = 0. \tag{5}$$

Since the internal forces produce no work in absence of elastic deformations, we specify a small rigid body motion:

$$\delta \boldsymbol{r} = \delta \bar{\boldsymbol{r}} + \delta \bar{\theta}\, \boldsymbol{k} \times \boldsymbol{r}, \quad \delta \theta = \delta \bar{\theta}, \tag{6}$$

with constant independent variations $\delta \bar{\boldsymbol{r}}$ and $\delta \bar{\theta}$, to obtain the balance equations:

$$\boldsymbol{Q}' + \boldsymbol{q} = \rho\, \ddot{\boldsymbol{r}}, \quad M' + m + \boldsymbol{k} \cdot (\boldsymbol{r}' \times \boldsymbol{Q}) = I\, \ddot{\theta}. \tag{7}$$

Backward-substitution in (5) yields the constitutive relation:

$$\delta \tilde{U} = \boldsymbol{Q} \cdot (\delta \boldsymbol{r}' - \delta\theta\, \boldsymbol{k} \times \boldsymbol{r}') + M\, \delta\theta', \tag{8}$$

which we now aim to write as a linear form with the variations of independent strain measures. For this sake, we introduce a promising candidate to account for axial and shear strains:

$$\boldsymbol{\Gamma} = \boldsymbol{r}' - \mathbf{P} \cdot \mathring{\boldsymbol{r}}', \tag{9}$$

and study the variation of its components in direction of the material basis vectors:

$$\delta\Gamma_\alpha = \delta \boldsymbol{r}' \cdot \boldsymbol{e}_\alpha + \boldsymbol{r}' \cdot \delta \boldsymbol{e}_\alpha + (\delta \mathbf{P} \cdot \mathring{\boldsymbol{r}}') \cdot \boldsymbol{e}_\alpha + (\mathbf{P} \cdot \mathring{\boldsymbol{r}}') \cdot \delta \boldsymbol{e}_\alpha. \tag{10}$$

With (2) and (3), this allows to rewrite (8) as:

$$\delta \tilde{U} = Q_\alpha\, \delta\Gamma_\alpha + M\, \delta\theta', \tag{11}$$

from which we conclude that the strain energy density is a function of the independent strain measures:

$$\Gamma_\alpha = (\boldsymbol{r}' - \mathbf{P} \cdot \mathring{\boldsymbol{r}}') \cdot \boldsymbol{e}_\alpha, \quad \kappa = \theta'. \tag{12}$$

For the considered cases with symmetric rectangular cross-sections and small strain magnitudes, a simple quadratic form suffices:

$$\tilde{U} = \frac{1}{2}\, a\, \kappa^2 + \frac{1}{2}\, b_\alpha\, \Gamma_\alpha^2, \tag{13}$$

where a, b_α denote the stiffness coefficients for bending, extension and shear. The generalised forces are obtained through partial differentiation of the strain energy density:

$$M = \frac{\partial \tilde{U}}{\partial \kappa} = a\, \kappa, \quad Q_\alpha = \frac{\partial \tilde{U}}{\partial \Gamma_\alpha} = b_\alpha\, \Gamma_\alpha. \tag{14}$$

This concludes the derivation of the governing set of equations for the Cosserat theory of shear-deformable rods, which comprises the above constitutive relations, the strain definitions (12) as well as the balance equations (7). It constitutes the most general formulation for the considered kind of planar rod theory with three particle degrees of freedom. That is to say, extended theories require a different assumption concerning the kinematic abilities of each material particle. For example, in the framework of the above utilized director formulation of rods with a co-rotating material basis, a length variation of the basis vector $\boldsymbol{e}_2$ could be considered as an additional degree of freedom. This would capacitate the corresponding non-classic rod to exhibit transverse normal strains, which may have a significant impact in problems involving contact, see [36, 37].

Emanating from the above deduced Cosserat theory of planar rods, we can easily switch to the alternative theories for unshearable rods or extensible strings by imposing certain kinematic constraints and considering some of the stiffness coefficients to vanish:

$$\text{unshearable rod:} \quad \Gamma_2 = 0 \tag{15}$$

$$\text{extensible string:} \quad a = 0, \quad b_2 = 0. \tag{16}$$

The condition $\Gamma_2 = 0$ constrains transverse shear and ensures that the tangential direction of the rod axis $\boldsymbol{r}'$ coincides with the normal direction of the cross-section $\boldsymbol{e}_1$. The ideally flexible string can bear neither bending moments nor transverse forces, which means that the balance of angular momentum in (7) can be disregarded. Any kinematic constraint reduces the number of available constitutive relations (14) by one. As a consequence of constrained transverse shear, the axial strain component simplifies to:

$$\Gamma_1 = |\boldsymbol{r}'| - 1, \tag{17}$$

which is known as Biot strain, as opposed to the Green strain measure:

$$\varepsilon = \frac{1}{2}\left(\boldsymbol{r}' \cdot \boldsymbol{r}' - 1\right). \tag{18}$$

The Biot-type is generally preferred for analytic studies, as it does not require the introduction of a conjugate generalised force to produce the same virtual work with $\delta\varepsilon$ as the axial force Q_1 does with $\delta\Gamma_1$. On the other hand, the quadratic nature of the Green-type makes it advantageous for the implementation in numerical simulation models. Both measures agree up to first order for small strains.

Semi-analytic solutions for the different belt-drive problems considered in the research articles are obtained by means of a numerical integration of a closed boundary value problem. In the context of belt drives, these problems consist of a number of individual solution segments, which fall into one of three categories: free span, sticking zone or sliding zone. The matching conditions at each transition point between two segments constitute the boundary conditions to determine the unknown integration constants as well as the positions of the transition points themselves (boundaries of each solution segment). Standard coordinate transformation techniques are used to reformulate the boundary value problem with unknown boundaries in a form applicable to standard purpose solvers. Simple homotopy strategies are employed to obtain solutions for problems, which are numerically ill-conditioned.

4. Nonlinear theory of shells with geometric imperfections

We refer to [35, 38, 39] for the derivation of the governing equations of classic shells and focus on the introduction of geometric imperfections as pre-strains in the elastic strain energy of a Kirchhoff–Love shell, which we specify as a quadratic form:

$$U = \frac{1}{2} \iint \left(A_1 \, (\mathrm{tr}\mathbf{E})^2 + A_2 \, \mathbf{E} \cdot \cdot \mathbf{E} + D_1 \, (\mathrm{tr}\mathbf{K})^2 + D_2 \, \mathbf{K} \cdot \cdot \mathbf{K} \right) \mathrm{d}\overset{*}{A}. \tag{19}$$

The area element $\mathrm{d}\overset{*}{A}$ relates to the unstressed initial configuration and the stiffness coefficients A_α and D_α define the elastic response to a membrane straining and bending of the structure, respectively. The corresponding strain tensors read:

$$\mathbf{E} = \frac{1}{2} \left(\mathbf{F}^{\mathrm{T}} \cdot \mathbf{a} \cdot \mathbf{F} - \overset{*}{\mathbf{a}} \right), \quad \mathbf{K} = \mathbf{F}^{\mathrm{T}} \cdot \mathbf{b} \cdot \mathbf{F} - \overset{*}{\mathbf{b}}, \tag{20}$$

with the deformation gradient tensor $\mathbf{F}$ as well as the first and second metric tensors $\mathbf{a}$, $\mathbf{b}$ and their counterparts of the initial configuration $\overset{*}{\mathbf{a}}$, $\overset{*}{\mathbf{b}}$.

For the sake of the introduction of geometric imperfections, we view the total deformation from the initial state to the actual one $\overset{*}{\boldsymbol{r}} \to \boldsymbol{r}$ as a two-step process $\overset{*}{\boldsymbol{r}} \to \overset{\circ}{\boldsymbol{r}} \to \boldsymbol{r}$ with an intermediate reference configuration $\overset{\circ}{\boldsymbol{r}}$, as depicted in Fig. 2. The membrane pre-straining of the simple rectangular reference configuration $\overset{\circ}{\boldsymbol{r}}$ is accomplished by the deformation gradient tensor $\overset{*}{\mathbf{F}}$ that accounts for the stretching of infinitesimal length elements $\mathrm{d}\overset{*}{s}$ to elements $\mathrm{d}s$ of uniform reference length. In the most general case, we imagine the initial state $\overset{*}{\boldsymbol{r}}$ to be composed of a sequence of arbitrarily shaped plate-stripes. With regard to steel belt drives, infinitesimal trapezoids suffice to account for a certain pre-tension level and to model a belt with side edges of different lengths, which is referred to as "camber" imperfection in practice, see *Paper E*.

The metric tensors are most concisely stated with the help of planar nabla operators, which we implicitly define by means of the total differential of a field f:

$$\mathrm{d}f = \mathrm{d}\overset{*}{\boldsymbol{r}} \cdot \overset{*}{\nabla} f, \quad \mathrm{d}f = \mathrm{d}\overset{\circ}{\boldsymbol{r}} \cdot \overset{\circ}{\nabla} f, \quad \mathrm{d}f = \mathrm{d}\boldsymbol{r} \cdot \nabla f. \tag{21}$$

The three operators $\{\overset{*}{\nabla}, \overset{\circ}{\nabla}, \nabla\}$ feature partial derivatives with respect to the material coordinates and are dedicated to the undeformed initial configuration, the pre-strained reference configuration and the deformed state, respectively. The corresponding metric tensors read:

$$\overset{*}{\mathbf{a}} = \overset{*}{\nabla} \overset{*}{\boldsymbol{r}}, \quad \overset{\circ}{\mathbf{a}} = \overset{\circ}{\nabla} \overset{\circ}{\boldsymbol{r}}, \quad \mathbf{a} = \nabla \boldsymbol{r}, \tag{22}$$

$$\overset{*}{\mathbf{b}} = -\overset{*}{\nabla} \overset{*}{\boldsymbol{n}}, \quad \overset{\circ}{\mathbf{b}} = -\overset{\circ}{\nabla} \overset{\circ}{\boldsymbol{n}}, \quad \mathbf{b} = -\nabla \boldsymbol{n}. \tag{23}$$

The unshearability constraint imposed by the Kirchhoff–Love theory requires the normal vector $\boldsymbol{n}$ to remain orthogonal to the deformed surface. This amounts to a C^1 continuity condition for the construction of consistent finite element approximations, which proves difficult to satisfy in the proposed mixed Eulerian–Lagrangian framework, see Sect. 7.2.

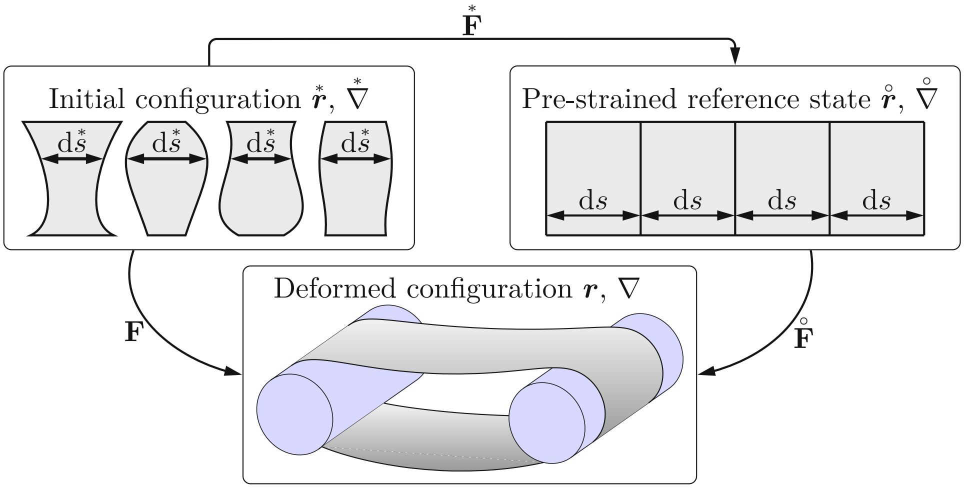

Figure 2: Introduction of geometric imperfections in the shell model: The initial state $\overset{*}{\boldsymbol{r}}$ comprises a sequence of infinitesimal plate stripes and induces strains in the rectangular reference configuration $\overset{\circ}{\boldsymbol{r}}$, which is deformed further to yield the actual state $\boldsymbol{r}$. This two-step process is accomplished through a multiplicative decomposition of the deformation gradient tensor $\mathbf{F}$.

The three kinds of deformation gradient tensors, which relate to the deformation steps visualised in Fig. 2, are stated as:

$$\overset{*}{\mathbf{F}} = \left(\overset{*}{\nabla}\overset{\circ}{\boldsymbol{r}}\right)^{\mathrm{T}}, \quad \overset{\circ}{\mathbf{F}} = \left(\overset{\circ}{\nabla}\boldsymbol{r}\right)^{\mathrm{T}}, \quad \mathbf{F} = \left(\overset{*}{\nabla}\boldsymbol{r}\right)^{\mathrm{T}}. \tag{24}$$

It is noteworthy that the specification of $\overset{*}{\mathbf{F}}$ already suffices to recover the metric $\overset{*}{\mathbf{a}}$ and, as demonstrated in the following, to substitute the differential operator $\overset{*}{\nabla}$. Thus, we do not require an explicit representation of the initial state $\overset{*}{\boldsymbol{r}}$, which we cannot provide for an incompatible choice anyway. To relate the above tensors, we evaluate the total differential of the position vectors of the actual and the reference state following (21):

$$\mathrm{d}\boldsymbol{r} = \mathrm{d}\overset{*}{\boldsymbol{r}} \cdot \overset{*}{\nabla}\boldsymbol{r} = \mathrm{d}\overset{\circ}{\boldsymbol{r}} \cdot \overset{\circ}{\nabla}\boldsymbol{r}, \quad \mathrm{d}\overset{\circ}{\boldsymbol{r}} = \mathrm{d}\overset{*}{\boldsymbol{r}} \cdot \overset{*}{\nabla}\overset{\circ}{\boldsymbol{r}}, \tag{25}$$

which, after substitution of the second in the first formula, yields the multiplicative decomposition of the total deformation gradient tensor, see [28, 29]:

$$\mathbf{F} = \overset{\circ}{\mathbf{F}} \cdot \overset{*}{\mathbf{F}}. \tag{26}$$

This formal decoupling of different parts of the complete deformation presents an easy way to incorporate geometric imperfections by means of intrinsic strains in a reference configuration $\overset{\circ}{\boldsymbol{r}}$, which, owing to its simple prescribed shape, is well suited for parametrisation with material coordinates. In all studies on belt drives conducted so far, we assumed the initial configuration $\overset{*}{\boldsymbol{r}}$ of the belt to be flat; an initial curvature as additional imperfection could be easily incorporated by a nontrivial choice for $\overset{*}{\mathbf{b}}$.

5. Mixed Eulerian–Lagrangian kinematic description of a belt drive

As the most general case studied so far, we shall focus on the mixed kinematic description for the three-dimensional belt drive setup used for parametrisation of shell finite elements in *Paper E*; the corresponding descriptions for the planar problems studied in the other articles follow by analogy. That said, the MEL-parametrisation of the position vector of the shell $\boldsymbol{r}$ is actually best illustrated with a planar projection of the belt drive system, see Fig. 3. The origin of the Cartesian spatial system $\{\boldsymbol{i}, \boldsymbol{j}, \boldsymbol{k}\}$ is placed in the centre between the two drums. The key to the MEL-description lies in an alternative parametrisation of space featuring the circumferential spatial coordinate σ as well as the transverse deflection ν and the lateral (out-of-plane) deflection z; the latter two describe a displacement in planes orthogonal to coordinate lines of σ. The corresponding unit directions $\{\boldsymbol{t}_g, \boldsymbol{n}_g, \boldsymbol{k}\}$ constitute an orthonormal basis. In this compound coordinate system, which alternates between two outer polar (cylindrical) and two inner Cartesian regions, the position vector of a material point of the shell reads:

$$\boldsymbol{r}(\sigma, \zeta) = \boldsymbol{g}(\sigma) + \nu(\sigma, \zeta)\, \boldsymbol{n}_g + z(\sigma, \zeta)\, \boldsymbol{k}, \tag{27}$$

where $\boldsymbol{g}(\sigma)$ follows the contour of a deflection-less belt, i.e. the geometric contour of the drive with length $L_{\text{geom}} = 2H + 2R\pi$, where R and H denote the drum radius and the drum centre-to-centre distance, respectively. Hence, instead of a parametrisation with the usual Lagrangian coordinate pair $\{s, \zeta\}$, the MEL description (27) defines $\boldsymbol{r}$ as a function of the looped spatial coordinate σ and the material width-coordinate ζ. Technically, this modification rests upon a coordinate transformation from the axial material coordinate s to its spatial counterpart σ:

$$s = S(\sigma, \zeta). \tag{28}$$

In the context of finite element kinematics this means that $\{s, \nu, z\}$ are considered as primary unknowns for which appropriate finite element approximations need to be constructed, whereas $\{\sigma, \zeta\}$ serve as parametrisation coordinates with correspondence to the local finite element coordinates $\{q_2, q_1\}$, respectively.

The elastic strain energy (19) is defined in terms of material derivatives of the primary variables:

$$\mathring{\partial}_s\{s, \nu, z\} = \left.\frac{\partial\{s, \nu, z\}}{\partial s}\right|_{\zeta=\text{const}}, \quad \mathring{\partial}_\zeta\{s, \nu, z\} = \left.\frac{\partial\{s, \nu, z\}}{\partial \zeta}\right|_{s=\text{const}}, \tag{29}$$

with the operator $\mathring{\partial}$, as opposed to its Eulerian–Lagrangian counterpart ∂:

$$\partial_\sigma\{s, \nu, z\} = \left.\frac{\partial\{s, \nu, z\}}{\partial \sigma}\right|_{\zeta=\text{const}}, \quad \partial_\zeta\{s, \nu, z\} = \left.\frac{\partial\{s, \nu, z\}}{\partial \zeta}\right|_{\sigma=\text{const}}. \tag{30}$$

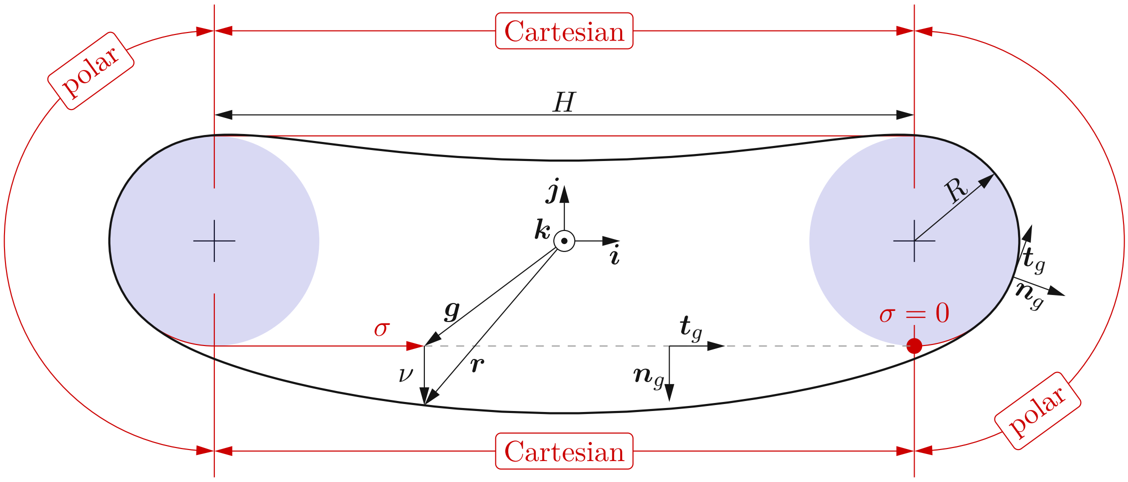

Figure 3: Mixed parametrisation of the shell position vector $\boldsymbol{r}$ featuring the spatial circumferential coordinate σ and the material width-coordinate ζ.

Likewise, we denote the total (material) and the local (spatial) time derivatives as:

$$\mathring{\partial}_t\{s,\nu,z\} = \left.\frac{\partial\{s,\nu,z\}}{\partial t}\right|_{s,\zeta=\text{const}}, \quad \partial_t\{s,\nu,z\} = \left.\frac{\partial\{s,\nu,z\}}{\partial t}\right|_{\sigma,\zeta=\text{const}}, \tag{31}$$

such that the total derivative of any field in MEL description can be split up into a convective and a local term, for example:

$$\mathring{\partial}_t s = 0 = \mathring{\partial}_t S = \partial_\sigma S \, \mathring{\partial}_t \sigma + \partial_t S. \tag{32}$$

In the special case of a steady state with constant material transport rate $\partial_t S = -c$ and a stationary distribution of material particles (time-invariance of $\partial_\sigma S$), we can integrate this equation in time with the initial condition $S(\sigma, \zeta, 0) = \xi$ to obtain:

$$S = \xi - \partial_\sigma \xi \, \mathring{\partial}_t \sigma \, t = \xi - c\, t. \tag{33}$$

For the particular choice $\sigma = \xi$, this kind of transformation to a time-invariant variable ξ is frequently applied in the literature for the analytical treatment of steady-state problems, see [40]. The above formulation emphasizes the difference of parametrisation with a truly spatial coordinate σ, in contrast to a hybrid coordinate ξ that inherits the stretching of material length elements ($\partial_\xi S = 1$).

In order to write the components of the metric tensors in terms of the derivatives with respect to the mixed parametrisation coordinates (30), we deduce some transformation formulas:

$$\begin{aligned} \mathring{\partial}_s s = 1 = \mathring{\partial}_s S = \partial_\sigma S \, \mathring{\partial}_s \sigma + \partial_\zeta S \, \mathring{\partial}_s \zeta, \\ \mathring{\partial}_\zeta s = 0 = \mathring{\partial}_\zeta S = \partial_\sigma S \, \mathring{\partial}_\zeta \sigma + \partial_\zeta S \, \mathring{\partial}_\zeta \zeta, \end{aligned} \tag{34}$$

which, due to $\mathring{\partial}_s\zeta = 0$ and $\mathring{\partial}_\zeta\zeta = 1$, simplifies to:

$$\mathring{\partial}_s\sigma = (\partial_\sigma S)^{-1}, \quad \mathring{\partial}_\zeta\sigma = -(\partial_\sigma S)^{-1}\,\partial_\zeta S. \tag{35}$$

With the material derivatives of the deflection variables $\{\nu, z\}$ in analogy to (34):

$$\mathring{\partial}_s\nu = \frac{\partial_\sigma\nu}{\partial_\sigma S}, \quad \mathring{\partial}_\zeta\nu = \partial_\zeta\nu - \frac{\partial_\zeta S}{\partial_\sigma S}, \quad \mathring{\partial}_s z = \frac{\partial_\sigma z}{\partial_\sigma S}, \quad \mathring{\partial}_\zeta z = \partial_\zeta z - \frac{\partial_\zeta S}{\partial_\sigma S}, \tag{36}$$

the sought-after material derivatives of the position vector $\boldsymbol{r}$ expand to:

$$\begin{aligned} \mathring{\partial}_s\boldsymbol{r} &= (1+\alpha\nu)\,\frac{1}{\partial_\sigma S}\,\boldsymbol{t}_g + \frac{\partial_\sigma\nu}{\partial_\sigma S}\,\boldsymbol{n}_g + \frac{\partial_\sigma z}{\partial_\sigma S}\,\boldsymbol{k}, \\ \mathring{\partial}_\zeta\boldsymbol{r} &= -\,(1+\alpha\nu)\,\frac{\partial_\zeta S}{\partial_\sigma S}\,\boldsymbol{t}_g + \left(\partial_\zeta\nu - \frac{\partial_\zeta S}{\partial_\sigma S}\partial_\sigma\nu\right)\boldsymbol{n}_g + \left(\partial_\zeta z - \frac{\partial_\zeta S}{\partial_\sigma S}\partial_\sigma z\right)\boldsymbol{k}. \end{aligned} \tag{37}$$

Here, we have introduced the piecewise constant α to denote the derivatives of the unit vectors $\{\boldsymbol{t}_g, \boldsymbol{n}_g\}$ of the geometric contour $\boldsymbol{g}$, see Fig. 3:

$$\partial_\sigma\boldsymbol{g} = \boldsymbol{t}_g, \quad \partial_\sigma\boldsymbol{t}_g = -\alpha\,\boldsymbol{n}_g, \quad \partial_\sigma\boldsymbol{n}_g = \alpha\,\boldsymbol{t}_g. \tag{38}$$

In particular, $\alpha = 0$ holds in the Cartesian and $\alpha = 1/R$ holds in the polar domains of the compound coordinate system. That is to say: α introduces a discontinuity of the metric at the coordinate transition lines, where σ switches from Cartesian to polar or vice versa. This poses a problem for the construction of consistent finite element ansatz functions, which need to fulfil the C^1 continuity requirement, i.e. the approximation of the position vector must be continuous up to (and including) its first order derivatives (37). The problem is overcome by means of augmented finite element approximations, see the concluding remarks in Sect. 7.2.

6. Contact modelling for belt drives

This section features a discussion of the different approaches to model contact in the proposed finite element schemes. It closes with some remarks regarding the behaviour of constrained structural theories in problems of solid contact.

6.1. Augmented Lagrangian multiplier approach for dry friction contact

The here studied problem of a looped belt in frictional contact with two rigid cylindrical drums may be formulated as a constrained variational problem: The principle of virtual work is accompanied by constraints, usually stated as Kuhn–Tucker conditions, see [22], to enforce the Coulomb frictional model.

The two traditional strategies to reach an unconstrained formulation that is accessible to standard finite element solvers are: the *penalty regularisation method* and the *Lagrange multiplier method*. The penalty regularisation procedure invokes high contributions to the total energy in case of a violation of the contact constraints. It is easy to implement and preserves the small bandwidth structure of the finite element system of equations, but it is inherently approximate and has a limited practical accuracy as high penalty factors induce numerical ill-conditioning. The Lagrangian multiplier method on the other hand incorporates the constraints directly into an extended system of equations. The introduction of the Lagrange multipliers enables an identical fulfilment of the contact constraints, but proves numerically inefficient owing to the enlarged system of equations and the loss of its favourable symmetric structure.

The *augmented Lagrangian multiplier method* combines the essential features of the two classic approaches and circumvents their drawbacks. At heart, it is a slightly extended penalty regularisation scheme that is accompanied by an outer-loop aimed at solving the original Lagrange multiplier problem by means of an iterative update of Lagrange multiplier estimates. The different variants of the augmented Lagrangian procedure employed for the treatment of Coulomb frictional contact in our research are based on the algorithm presented in Tab. 1 and originally proposed in [23]. It features rules for the detection of the contact state, the evaluation of the contact tractions as well as the update of the Lagrange multiplier estimates. Contact detection, which amounts to the evaluation of the penetration depth γ, is trivial for the pairing of a rigid cylindrical drum with a belt wrapped around it, but is generally considered one of the primary challenges of contact modelling, again see [22]. A positive penetration γ of the belt into the drum surface invokes a contact pressure τ_γ with a penalty factor P_γ.

The tangential contact is resolved by means of a return-mapping algorithm that is frequently applied to problems of frictional contact and metal plasticity, see for example [41]. It introduces an auxiliary traction vector $\overset{*}{\boldsymbol{\tau}}$ under the assumption of stick to evaluate the friction criterion Φ (yield function). If $\Phi < 0$ holds, i.e. the trial-state remains within the Coulomb friction cone (yield surface), $\overset{*}{\boldsymbol{\tau}}_\perp$ equals the actual traction. Sliding is detected with $\Phi \geq 0$ and the return-mapping scheme is invoked to ensure that $\boldsymbol{\tau}_\perp$ comes to rest on the friction cone; the unit direction $\boldsymbol{e}$ of the auxiliary vector $\overset{*}{\boldsymbol{\tau}}_\perp$ determines the sliding direction. It is noteworthy that the above introduced frictional tractions $\boldsymbol{\tau}_\perp$ are aligned with the tangential displacements $\boldsymbol{u}$ and, thus, point in opposite direction of the physical tractions; obviously, this holds for $\overset{*}{\boldsymbol{\tau}}_\perp$ and $\boldsymbol{\lambda}_\perp$ alike.

	normal contact	sticking contact	sliding contact
detection	$\gamma > 0$	$\Phi < 0$	$\Phi \geq 0$
evaluation	$\tau_\gamma = \lambda_\gamma + P_\gamma \gamma$	$\boldsymbol{\tau}_\perp = \overset{*}{\boldsymbol{\tau}}_\perp$	$\boldsymbol{\tau}_\perp = \eta \tau_\gamma \boldsymbol{e}$
update	$\lambda_\gamma \leftarrow \lambda_\gamma + P_\gamma \gamma$	$\boldsymbol{\lambda}_\perp \leftarrow \boldsymbol{\lambda}_\perp + P_\perp \boldsymbol{u}$	$\boldsymbol{\lambda}_\perp \leftarrow \eta \tau_\gamma \boldsymbol{e}$
	with $\Phi = \lvert\overset{*}{\boldsymbol{\tau}}_\perp\rvert - \eta\tau_\gamma$,	$\overset{*}{\boldsymbol{\tau}}_\perp = \boldsymbol{\lambda}_\perp + P_\perp \boldsymbol{u}$,	$\boldsymbol{e} = \frac{\overset{*}{\boldsymbol{\tau}}_\perp}{\lvert\overset{*}{\boldsymbol{\tau}}_\perp\rvert}$

Table 1: Contact detection, evaluation and update scheme for the augmented Lagrangian modelling strategy

The update of the Lagrangian multiplier estimates λ_γ and $\boldsymbol{\lambda}_\perp$ resembles a simple fixed point iteration scheme. The current estimates augment the penalty formulation of the traction components and are regarded constant in the principle of virtual work that features the contact contributions:

$$\delta V_\gamma = \iint\limits_{\gamma>0} \tau_\gamma \, \delta\gamma \, J \, \mathrm{d}\sigma \, \mathrm{d}\zeta, \quad \delta V_\perp = \iint\limits_{\gamma>0} \boldsymbol{\tau}_\perp \cdot \delta \boldsymbol{u} \, J \, \mathrm{d}\sigma \, \mathrm{d}\zeta, \tag{39}$$

which are written as variations of potentials and feature the Jacobian determinant J, whose specification depends on whether the contact forces should be counted per unit of reference area or per unit of actual area. For the lack of a better term, we refer to V_γ and $V_\perp$ as "potentials" owing to their immediate connection to the virtual work of the contact forces, however: $V_\perp$ is non-conservative with the source of energy dissipation relating to either Reynold's belt creep theory in case of dry friction contact or Firbank's shear theory in case of the regularised elastic contact model discussed in Sect. 6.2. In addition, contact establishment is detected with $\gamma > 0$ to exclude non-contacting areas, which means that the derivative $\partial V_\gamma / \partial \gamma$ is not unique at the boundary $\gamma = 0$.

The numerical solution of the variational problem via Newton iterations and the update of Lagrangian multiplier estimates alternate each other to obtain the solution for a single load or time increment by means of convergence of the fixed point iteration scheme. However, in some cases divergence is likely and a satisfactory convergence rate is difficult to achieve. In particular, the here studied belt drive problems prove challenging owing to the particularities of the contact response of constrained structural theories, to be discussed in Sect. 6.3, as well as due to the adverse parameter setting of a slack belt with high membrane stiffness. Though modifications to the basic scheme to remedy these issues are reported in the literature [42], we either revert to the basic penalty regularisation method or employ alternative integration rules in axial direction to promote convergence, see Sect. 7.3. The corresponding penalty regularisation scheme is easy to retrieve from Tab. 1 by setting $\lambda_\gamma = \boldsymbol{\lambda}_\perp = 0$.

6.2. Regularised elastic contact model for steel belt drives

Convergence of the augmented Lagrangian contact approach, as presented at the 2019 annual meeting of GAMM, see [43], is difficult to achieve in the parameter range of a slack steel belt. Therefore, we propose a simplified elastic contact model with full neglect of sliding friction. It is based on the notion of an elastic interlayer to transfer the contact forces between deformable belt and rigid drums and resembles the practically relevant case of drums with a polymer wrapping. The good correspondence to the experimental results obtained for steel-to-steel contact, as reported in *Paper E*, justifies the usage of this substitutional model as a numerically robust alternative to other approaches that aim at the exact enforcement of the dry friction contact constraints.

The effective stiffness coefficients of the intermediate layer, which are determined through a study of simple deformation cases of a sample piece depicted in Fig. 4 under the assumption of small strains and a linear elastic constitutive behaviour, are inverse proportional to the layer thickness d. Hence, the elastic response in case of a thin layer with the contact potentials:

$$V_\gamma = \frac{1}{2} \iint\limits_{\gamma>0} P\,\gamma^2\,J\,\mathrm{d}\sigma\,\mathrm{d}\zeta, \quad V_\perp = \frac{1}{2} \iint\limits_{\gamma>0} P_\perp\,\boldsymbol{u}\cdot\boldsymbol{u}\,J\,\mathrm{d}\sigma\,\mathrm{d}\zeta, \tag{40}$$

is closely related to a penalty regularisation procedure to enforce a pure-stick solution; the stiffness coefficients of the wrapping P and $P_\perp$ relate to penalty factors.

Contrary to the classic penalty regularisation, we need to account for the transport of the shear deformations of the interlayer in axial direction (the wrapping is transported with the drum). This gives rise to convective terms in the partial differential equation for the field of the tangential deformations in mixed kinematic description $\boldsymbol{u} = \boldsymbol{u}(\sigma, \zeta)$:

$$\partial_t \boldsymbol{u} = \left(\mathring{\partial}_t \boldsymbol{r} - \mathring{\partial}_t \boldsymbol{R}\right)_\perp - \partial_\sigma \boldsymbol{u}\,\mathring{\partial}_t \sigma, \tag{41}$$

where $\perp$ denotes a projection of 3D-vectors onto the tangential contact plane and $\boldsymbol{R}$ represents the position vector of the dedicated point on the drum surface that coincided with the shell position vector $\boldsymbol{r}$ at the instance of contact establishment. The notion of dedicated particles whose different trajectories determine the deformation of the interlayer is sometimes referred to as *brush-model* in the literature [31]. The above advection problem is responsible for the axial motion of the belt as it introduces the prescribed angular velocity via $|\mathring{\partial}_t \boldsymbol{R}| = \omega$. The additional convective term on the right would be absent in the case of dry-friction contact, that is to say: the sliding velocity of a single point is fully determined by the difference of the velocities of the dedicated particles. A semi-implicit finite difference scheme with a finite time step Δt is applied to incorporate the above advection problem into the finite element system of equations.

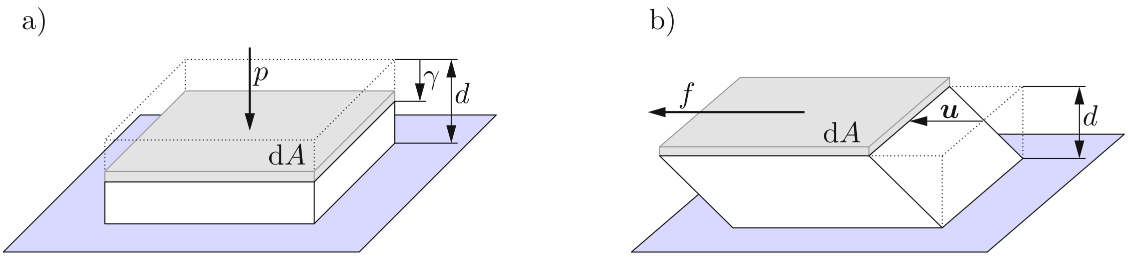

Figure 4: Simple deformation cases of a sample piece of the elastic interlayer with thickness d to conclude on the effective stiffness coefficients.

6.3. Remarks on the treatment of contact problems with constrained structural theories

Constrained theories of structures exhibit a distinct behaviour when applied to solid contact problems that does not always conform to the corresponding response of the solid continuum body. This comes as no surprise, as the classic theories in the framework of the asymptotic approach are obtained for the free part of the structure in a safe distance to the boundaries; the so-called edge layer requires a different series expansion, see [44, 45]. Hence, when pursuing a unified approach to model the belt in the free span regions as well as the contact zones with a single constrained theory, we must be aware that the structure may not produce consistent results at the boundaries between the domains.

It is well known that both the Cosserat theory of rods as well as the corresponding unshearable theory, obtained by imposing the constraint of shear-rigidity (15), produce an unphysical distribution of the contact pressure τ_γ in proximity to the points of first and last contact as compared to the solution of the contact problem for the elastic continuum, see [25, 46, 47]. In particular, τ_γ should vanish at the contact zone boundaries, but it remains finite for the Cosserat theory, see *Paper D*, and becomes unbounded for the unshearable theory, see *Paper A*; the Kirchhoff–Love shell behaves just like the unshearable rod, see *Paper E*. The discontinuity of the transverse force arising for the unshearable theory is illustrated in Fig. 5a for the geometrically linearised problem of an initially straight rod that is pre-tensioned with an axial force F and stands in frictionless contact with a rigid stamp, see *Paper A* for the solution in the framework of the incremental rod theory [35]; the corresponding solution for the Cosserat theory is visualised in Fig. 5b. Research conducted for different types of constrained rod theories revealed that the neglect of transverse normal strains of the above classic theories is responsible for the peculiar normal contact response. In other words: The incorporation of transverse normal strains in an extended theory, which in the context of the director formulation of rods relates to a length variation of the transverse unit vector $\boldsymbol{e}_2$ in (1), permits a consistent distribution of the normal contact pressure, see [36, 37].

The coupling of normal and tangential contact forces in the sliding region for the Coulomb frictional model induces concentrated contributions in the tangential component $\boldsymbol{\tau}_\perp$ close to the run-off edge, where the belt leaves the contact zone; the tangential deformation $\boldsymbol{u}$ exhibits corresponding peaks for the regularised elastic model described in Sect. 6.2. Fine time steps and a locally refined mesh are required to resolve these particularities, which is crucial owing to their immediate connection to a membrane straining of the belt. In addition, the high gradients of the contact tractions at the contact zone boundaries present a hindrance for the convergence of the iterative augmented Lagrangian multiplier method, see Sect. 6.1; modified integration rules alleviate this issue to some degree, see Sect. 7.3.

Though rod-to-surface frictional contact problems are not considered here, it is worth mentioning another peculiarity arising in case of a partial transverse sliding motion of an unshearable rod: As reported in [48], the solution in the slip zone of a heavy semi-infinite Bernoulli–Euler beam resting on a rough plane surface with transverse loading at the tip

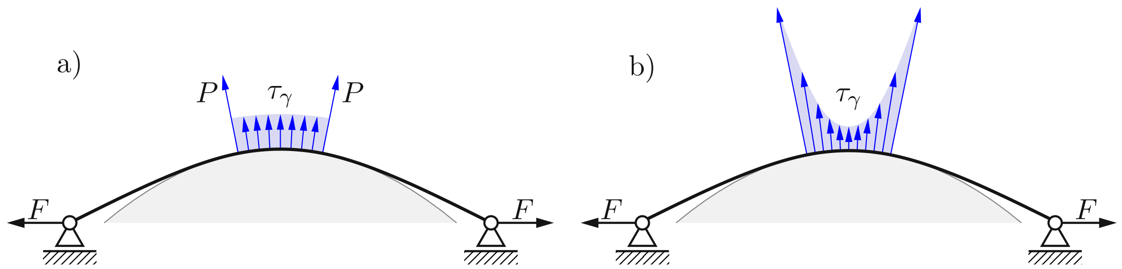

Figure 5: Geometrically linearised problem of a rod in contact with a rigid stamp and pre-tensioned by an axial force F: a) Unshearable rod theory: The normal contact response features a constant pressure τ_γ in the interior and concentrated contributions P at the boundaries; b) Cosserat theory: The contact pressure τ_γ is maximal at the boundaries and tends to Dirac-discontinuities in the limiting case of vanishing shear compliance.

features an infinite number of self-similar solution regimes with alternating direction of the frictional force. The practical example of inhomogeneous cooling of long rails on a rough surface after thermal treatment is considered in [49], and [50] establishes the same kind of solution for an axially moving beam travelling across a rough surface.

Another aspect worth mentioning is the impact of the action line of frictional forces on the solution of the belt drive problem, see [51–53]. The account for an eccentric action of the tangential tractions gives rise to distributed bending moments $m \neq 0$ in the balance equation (7) of the rod theory. For simplicity and justified by the thinness of the belt in the considered examples, we assume the frictional forces to act on the centre fibre.

7. Finite element related aspects

In this section we address the actual computation of finite element solutions, remark on the construction of consistent finite element approximations and discuss the implementation of mixed integration rules to remedy certain numerical issues.

7.1. Finite element solution of the contact problem

In the most general case, we seek a stationary value of the Lagrangian L:

$$\delta L = \delta U + \delta W + \delta V_\gamma + \delta V_\perp - \delta T = 0 \tag{42}$$

which corresponds to the formulation of Hamilton's principle for stationary processes [54]. Owing to the automatic conservation of mass in the considered belt drive problems, the above formula remains unchanged upon introduction of the MEL kinematic description; corresponding modifications are necessary for open systems with changeable mass, see [55, 56]. The contributions of the persistent inertia terms introduced through the kinetic energy T are neglected frequently, in which case we simply seek a minimum of the total potential energy comprising the elastic strain energy U, the potential of gravity W as well as the contact potentials for normal contact V_γ and tangential contact $V_\perp$.

The equations for increments of the nodal degrees of freedom in the displacement based MEL finite element framework are solved with a standard Newton algorithm. Static configurations of the hanging belt (no drum rotation, $\omega = 0$) are computed with a homotopy procedure that follows the solution path from tight configurations with negligible transverse deflections to slack states with weak belt-tension and large sag. The quasistatic transient motion is simulated as a sequence of minima of the total potential energy; prescribed increments of the drum rotation $\omega\Delta t$ transport the belt in axial direction.

The belt has adopted a stationary state, if its deformed configurations at different times t_1 and t_2 are visually indistinguishable, while the particles keep travelling through this statically deflected state with a constant rate of material transport. In the proposed mixed Eulerian-Lagrangian finite element kinematic description, this corresponds to time-invariant solution in the primary variables.

7.2. Construction of finite element approximations

The approximations for the two-node rod finite element models are based on the linear combination of nodal variables with the cubic ansatz functions:

$$\begin{aligned} \psi_1(\xi) &= \frac{1}{4}(\xi-1)^2(\xi+2), \quad \psi_2(\xi) = \frac{1}{4}(\xi-1)^2(\xi+1), \\ \psi_3(\xi) &= \frac{1}{4}(\xi+1)^2(-\xi+2), \quad \psi_4(\xi) = \frac{1}{4}(\xi+1)^2(\xi-1). \end{aligned} \tag{43}$$

The shape functions with odd indices relate to the value of a primary unknown at the nodal points $\xi = \pm 1$ and those with even indices define the nodal derivatives with respect to the local coordinate ξ. The total number of degrees of freedom of a single element depends on the employed structural theory.

The corresponding bi-cubic polynomials, originally proposed in [57] for plate bending problems, for the discretisation of a field in the shell finite element model can be constructed as products of these elementary functions. For example, Fig. 6 depicts the four ansatz functions for the first node with local coordinates $q_1 = q_2 = -1$ in the shell model, defined as:

$$\begin{aligned} \Psi_1 &= \psi_1(q_1)\,\psi_1(q_2), \quad \Psi_2 = \psi_2(q_1)\,\psi_1(q_2), \\ \Psi_3 &= \psi_1(q_1)\,\psi_2(q_2), \quad \Psi_4 = \psi_2(q_1)\,\psi_2(q_2), \end{aligned} \tag{44}$$

which, in order of appearance, correspond to the value of the field itself, its first derivative with respect to q_1 and q_2 as well as the mixed second order derivative. The latter is not strictly required for satisfaction of the C^1 continuity constraint imposed by the Kirchhoff–Love theory, but guarantees that any bi-cubic polynomial can be approximated and, thus, contributes to the completeness of the approximation, see [35, 58]. A single four-node shell finite element with the primary variables $\{s, \nu, z\}$ features a total of $4 \times 4 \times 3 = 48$ degrees of freedom.

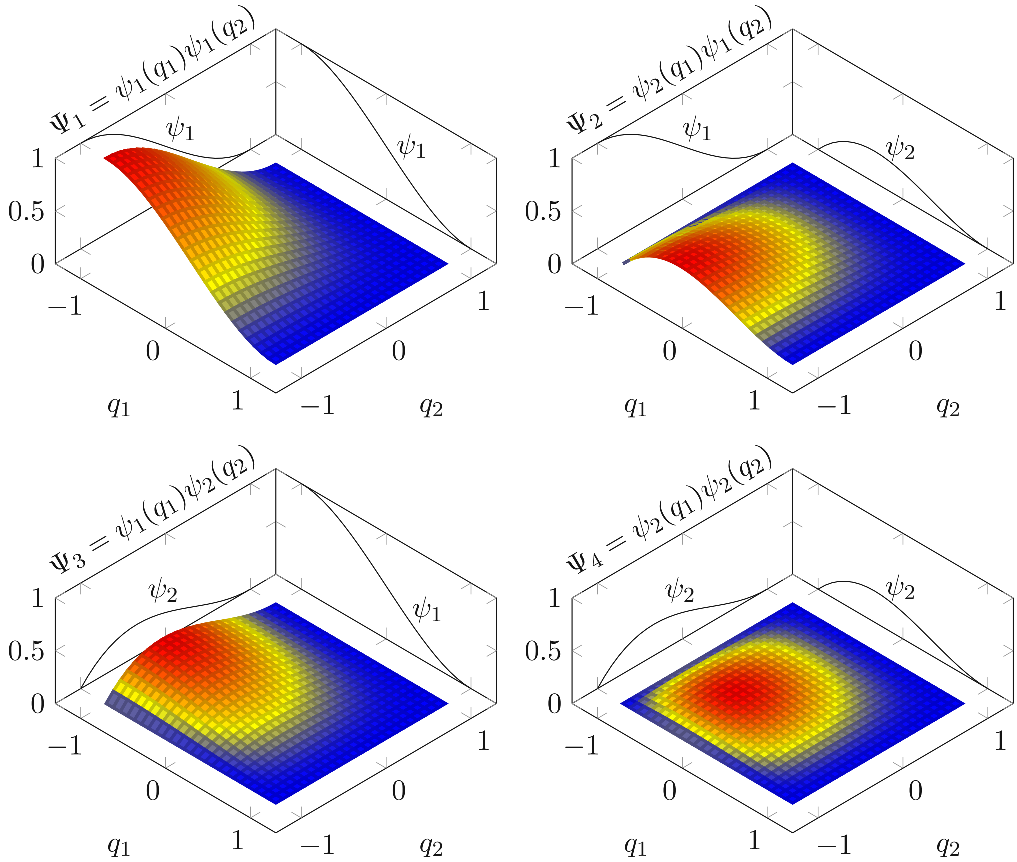

Figure 6: Basic bi-cubic shape functions Ψ_i of the first nodal point constructed as products of the elementary cubic polynomials ψ_i.

The originally provided C^1 continuity is lost as a consequence of the MEL kinematic description owing to a discontinuity of the metric of the compound coordinate system. Specifically, the derivatives of the unit vectors $\boldsymbol{t}_g$ and $\boldsymbol{n}_g$ become discontinuous at the coordinate transitions of the circumferential coordinate σ, see Fig. 3. Extended approximations based on the above basic ansatz functions are constructed to overcome this issue. The presence of the width coordinate ζ significantly complicates this process for the shell model of the belt. As an inconvenient side effect, the augmented approximations become quadratic in the nodal unknowns, which makes the computation of analytic derivatives cumbersome.

7.3. Evaluation of element energies and mixed integration rules

As usual, numerical integration routines are applied for the evaluation of finite element contributions to the total potential energy. Though preferred for accuracy reasons in general, see [59], application of Gaussian quadrature rules in axial direction is problematic, because it promotes membrane locking and endangers the convergence of the contact forces in the augmented Lagrangian scheme. Both issues are a consequence of the limited kinematic abilities of the finite element approximations. As a thorough remedy, we shall consider an enriched kinematic approach based on the isogeometric analysis in the future, see [60, 61]; here we rely on the comparatively simple countermeasure of modified integration schemes.

To illustrate the numerical phenomenon of membrane locking, we study the deformation of an initially straight leaf spring to a semi-circle of the same length:

$$\mathring{\boldsymbol{r}} = s\,\boldsymbol{i}, \quad \boldsymbol{r} = R\,\sin\left(\frac{s}{R}\right)\boldsymbol{i} + R\left(\cos\left(\frac{s}{R}\right) - 1\right)\boldsymbol{j}, \quad s \in [0, R\pi]\,. \tag{45}$$

The axial strains, see (17), vanish identically

$$\Gamma_1 = |\boldsymbol{r}'| - 1 = 0, \tag{46}$$

but the corresponding Cartesian finite element approximation with a single element in the domain of the local coordinate $\xi \in [-1, 1]$ with the basic cubic shape functions (43) fails to reproduce this result. From Fig. 7 we conclude that the axial strains are best sampled at the coordinates $\xi = \{-1, 0, 1\}$, which corresponds to the Simpson quadrature rule; three points are required to avoid spurious deformations (hour-glassing because of the under-constraining).

The ability of a displacement based finite element scheme to accurately predict certain strain states depends on the level of distortion with respect to the element's undeformed reference state. In regard to the MEL finite elements in the compound coordinate system, see Fig. 3, the phenomenon of membrane locking is most pronounced in proximity to coordinate transition points, where the finite element parametrisation switches between Cartesian and polar; i.e. initially curved polar elements are straightened and initially straight Cartesian elements in the contact zone are bent to fit the drum's curvature. Since the shell finite elements essentially retain their initial shape in lateral direction, it is appropriate to resolve the width direction with the standard three-point Gauss rule. The proposed mixed integration scheme for the membrane energy of a shell finite element is presented in Fig. 8a. It resembles more evolved MITC-strategies that feature independent interpolations for the strains, which are connected to the displacement derived strains at so-called tying points, see [62].

The standard integration routine to evaluate the work contributions of the contact forces (39) in the shell model is a 2×2 Gaussian quadrature rule. Lagrange multiplier estimates and the information concerning the frictional contact state are stored for every integration point. However, in regard to the above mentioned convergence issues, the mixed integration rule depicted in Fig. 8b, which employs the trapezoidal rule to place the integration points on the element edges, is advantageous with the following reasoning: The kinematic limitations of the element ansatz functions prevent the perfect adhesion to the drum surface ($\gamma = 0$) in the interior of an element, see Fig. 7a, whereas evaluation at the element edges in axial direction allows for a compliant deformation, thanks to the immediate connection of γ to the nodal variables.

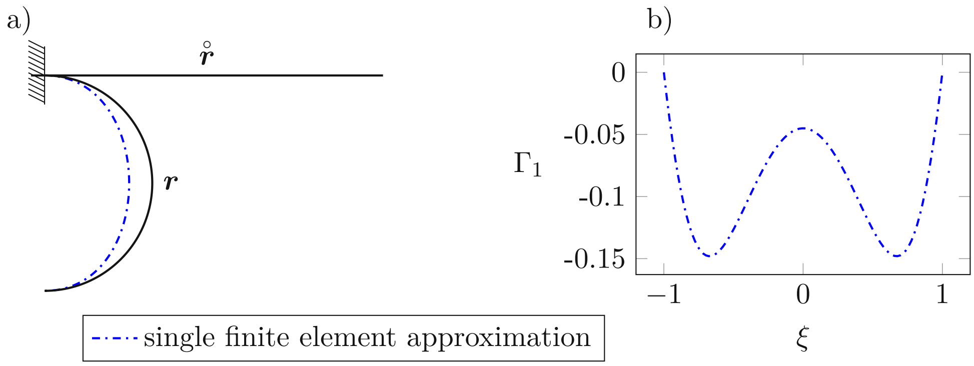

Figure 7: On the phenomenon of membrane locking: a) Simple deformation of an initially straight leaf spring to a semi-circle and its approximation by means of a single Cartesian finite element; b) to reproduce the analytic solution $\Gamma_1 = 0$ most accurately, the finite element strains are best sampled at the points $\xi = \{-1, 0, 1\}$, which corresponds to the Simpson rule of integration.

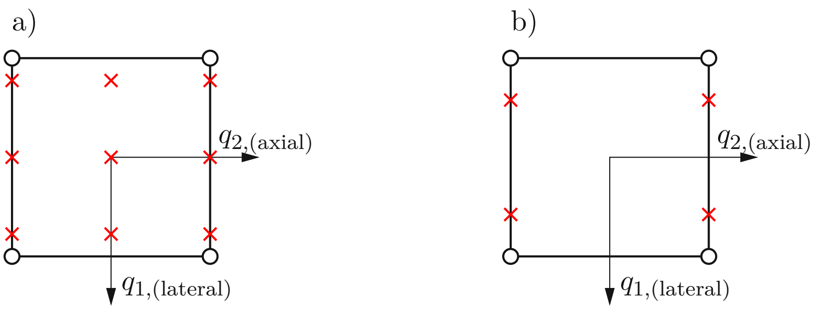

Figure 8: Mixed integration rules: a) Simpson rule in axial direction and three-point Gauss formula in lateral direction for the membrane energy; b) trapezoidal rule and two-point Gauss formula in lateral direction for the contact potentials.

The contact resolution with the two-point Gauss scheme in width direction in the shell model is less critical, because of the essentially straight line of contact in this direction. Naturally, in case of a significant misalignment of element edges and drum surface in lateral direction, for example due to a large tilting motion of the drum or a profiled drum shape, the integration scheme should be adapted accordingly.

8. Summary of the journal articles

8.1. Paper A

Flexible belt hanging on two pulleys: Contact problem at non-material kinematic description

Yury Vetyukov, Evgenii Oborin, Jakob Scheidl,
Michael Krommer, Christian Schmidrathner

International Journal of Solids and Structures
https://doi.org/10.1016/j.ijsolstr.2019.03.034

In this publication, we establish the MEL kinematic formulation of rod finite elements in the benchmark problem of a planar two-pulley belt drive, which requires the definition of extended finite element approximations to compensate for the discontinuous metric of the compound coordinate system. The discussion is limited to the static solution of the belt hanging in frictionless contact with the circular pulleys. The normal contact response is modelled with a standard penalty regularisation scheme and the phenomenon of membrane locking in proximity to the coordinate transitions of the compound coordinate system is observed for coarse finite element discretisation levels. A novel solution obtained through numerical integration of the corresponding symmetric boundary value problem and comparative simulations with standard Lagrangian finite elements demonstrate consistency and numerical efficiency of the MEL scheme.

Jakob Scheidl is responsible for: writing of the original draft; numerical validation; parameter studies and comparative computations; visualisation and presentation of the results at the GAMM annual conference 2018, see [63].

8.2. Paper B

Motion of a friction belt drive at mixed kinematic description

Jakob Scheidl

International Journal of Solids and Structures
https://doi.org/10.1016/j.ijsolstr.2020.05.001

In continuation of the research covered in *Paper A*, we simulate the transient axial motion of the belt with MEL finite elements based on the structural model of an extensible string. Full transient dynamics are disregarded in the proposed quasistatic scheme, but stationary inertia contributions that persist after the transient effects have subsided are considered. The augmented Lagrangian procedure is employed to treat the Coulomb frictional contact, which amounts to a belt creep theory type of solution in the pulley contact zones. The finite element results are verified against semi-analytic solutions obtained for the stationary motion problem. In resemblance of the compound coordinate system of the MEL description, the boundary value problem utilizes a piecewise spatial parametrisation of the primary variables; the formulation is easily extendable to multi-pulley belt drive problems.

Jakob Scheidl is the sole author.

8.3. Paper C

Steady motion of a belt in frictional contact with a rotating pulley

Jakob Scheidl, Yury Vetyukov — Dynamics and Control of Advanced Structures and Machines
https://doi.org/10.1007/978-3-030-79325-8_18

In this peer-reviewed book chapter, we introduce a novel concept to seek the stationary finite element solution of an axially moving structure directly, that is, without the need to run through a transient process. In particular, we study the planar problem of a belt that is transported over a single pulley while passing through an open domain at a constant material transport rate. We employ the standard transformation formula (33) to reach a time-invariant parametrisation for the finite element scheme. The applied Cosserat theory of rods avoids discontinuous jumps of the transverse force and, thus, contributes to the convergence of the iterative augmented Lagrangian contact procedure to treat the Coulomb dry friction contact. In an effort to ease the solution process, we assume a belt creep theory kind of solution from the very beginning and impose the position of the stick-to-slip transition point directly, in contrast to the usual approach with prescribed angular velocity of the pulley. Cartesian and polar parametrisations of the primary variables are used to formulate the corresponding boundary value problem, which is restated with normalised coordinates to make it accessible to standard purpose solvers. Finite element simulations are validated against the quasi-converged semi-analytic solutions.

Jakob Scheidl is responsible for: writing of the original draft; derivation of the analytic boundary value problem and its numerical solution; parameter studies involved in the validation of the finite element scheme.

8.4. Paper D

Steady motion of a slack belt drive: Dynamics of a beam in frictional contact with rotating pulleys

Jakob Scheidl, Yury Vetyukov — ASME Journal of Applied Mechanics
https://doi.org/10.1115/1.4048317

This article adapts the novel steady-state solution concept, originally proposed in *Paper C*, to the standard benchmark problem of the planar two-pulley belt drive, previously considered in *Paper A* in terms of the static deflection problem and *Paper B* with regard to the transient quasistatic motion. In analogy to *Paper C*, we employ the Cosserat theory of rods, assume a belt creep theory type of solution, and apply the iterative augmented Lagrangian procedure to treat Coulomb frictional contact in the MEL finite element framework. As concluded from the semi-analytic reference solution of the boundary value problem, prescribing the stick-to-slip transition points on both drums amounts to an overdetermined system of equations. In response to this observation, we seek the finite element solution by means of an iterative strategy involving an auxiliary problem that reduces to the original one upon fulfilment of a matching condition. The publication features a rigorous validation of the finite element scheme in comparison to the semi-analytic results, extensive parameter studies and remarks on the construction of consistent finite element approximations for Cosserat rods in the MEL kinematic description.

Jakob Scheidl is responsible for: writing of the original draft; implementation of the steady-state solution concept and the Cosserat theory of rods in the existing MEL finite element model of the two-pulley belt drive; derivation and numerical integration of the corresponding boundary value problem; validation of the finite element scheme in comparison to the semi-analytic results; execution of parameter studies.

8.5. Paper E

Mixed Eulerian–Lagrangian shell model for lateral run-off in a steel belt drive and its experimental validation

Jakob Scheidl, Yury Vetyukov, Christian Schmidrathner, Klemens Schulmeister, Michael Proschek

International Journal of Mechanical Sciences
https://doi.org/10.1016/j.ijmecsci.2021.106572

Compliant with the research goals of the industrial research project *LaLaBand*, this article covers the implementation and experimental validation of a geometrically nonlinear shell finite element scheme in the MEL kinematic framework to simulate the lateral run-off of a slack steel conveyor belt. Essential geometric imperfections of the belt are introduced as intrinsic strains in the reference configuration and tilting actions of the steering drum are considered as a means to counteract the lateral run-off. For the sake of computational efficiency, we employ a substitutional elastic contact model and mixed integration rules to remedy numerical issues related to membrane locking, the particularities of the contact response in the unshearable Kirchhoff–Love theory as well as the extreme membrane stiffness of the thin steel belt. Augmented shape functions are introduced to satisfy the C^1 continuity requirement for the MEL parametrisation with the circumferential coordinate σ and the material width coordinate ζ. Numerical studies are conducted to verify the convergence of the finite element scheme and to reproduce practically relevant results with regard to the phenomenon of lateral run-off. The good correspondence to a series of physical experiments demonstrates the ability of the finite element scheme to accurately capture the phenomenon of lateral run-off in a steel belt drive.

Jakob Scheidl is responsible for: writing of the original draft; implementation of geometric imperfections as intrinsic strains; contact modelling; account for misaligned drum axes; development of a multi-step simulation strategy; extensive code testing and parameter studies; acquiring and processing of experimental data; development of a validation strategy for the comparison against physical experiments.

9. Scientific impact

The cumulative thesis establishes a numerically efficient kinematic description, which incorporates the mixed Eulerian–Lagrangian approach in a looped compound coordinate system, for the finite element simulation of slack belt drives. Novel finite element schemes featuring unified structural models of the belt as a string, a rod or a shell are developed and validated by means of numerical convergence studies and comparison against semi-analytic reference solutions or physical experiments. A new concept for the immediate computation of the steady-state motion in the finite element framework is developed, in an effort to avoid the time consuming simulation of a transient process.

Various models for the numerical treatment of belt-to-pulley contact in the MEL framework are introduced. We pursue augmented Lagrangian multiplier or penalty regularisation strategies to enforce the constraints of Coulomb dry frictional contact and, in resemblance of belt shear theory, rely on an approximative elastic model for the numerically challenging simulation of a steel belt drive.

Novel semi-analytic solutions for the statically deflected configuration or the belt at stationary motion are obtained with account for large transverse deflections in the field of gravity and persistent inertia effects. The numerical solutions of the boundary value problems deduced for the different planar theories of rods are computed in a traditional manner utilizing alternative parametrisation strategies that emphasise the difference of material (Lagrangian) and spatial (Eulerian) descriptions. The numerical analysis for a Cosserat type of rod in the limiting case of vanishing shear compliance lets us conclude on the appropriate boundary conditions for the unshearable theory.

The application oriented part of the research in the framework of the industrial cooperation project *LaLaBand* focuses on the simulation of the lateral run-off in a slack steel belt drive. The corresponding shell finite element model is based on the MEL kinematic description, accounts for intrinsic geometric imperfections of the belt as well as misaligned drum axes and, as the comparison of simulation results against physical experiments demonstrates, is capable of an accurate estimation of the lateral run-off. It shall aid the industrial partner in the improvement of the production process of steel belts and provides a solid basis for the development of advanced designs for an active control of the lateral run-off.

References

[1] S. E. Bechtel et al. The Stretching and Slipping of Belts and Fibers on Pulleys. *Journal of Applied Mechanics* 67.1 (1999), 197–206. DOI: 10.1115/1.321164.

[2] M. B. Rubin. An Exact Solution for Steady Motion of an Extensible Belt in Multipulley Belt Drive Systems. *Journal of Mechanical Design* 122.3 (2000), 311–316. DOI: 10.1115/1.1288404.

[3] T. Firbank. Mechanics of the belt drive. *International Journal of Mechanical Sciences* 12.12 (1970), 1053–1063. DOI: https://doi.org/10.1016/0020-7403(70)90032-9.

[4] C. Mote. Divergence buckling of an edge-loaded axially moving band. *International Journal of Mechanical Sciences* 10.4 (1968), 281–295. DOI: https://doi.org/10.1016/0020-7403(68)90013-1.

[5] M. H. Ghayesh and M. Amabili. Post-buckling bifurcations and stability of high-speed axially moving beams. *International Journal of Mechanical Sciences* 68 (2013), 76–91. DOI: https://doi.org/10.1016/j.ijmecsci.2013.01.001.

[6] Y. Wu, M. J. Leamy and M. Varenberg. Belt-Drive Mechanics: Friction in the Absence of Sliding. *Journal of Applied Mechanics* 86.10 (2019). DOI: 10.1115/1.4044019.

[7] J. Synka and A. Kainz. A novel mixed Eulerian–Lagrangian finite-element method for steady-state hot rolling processes. *International Journal of Mechanical Sciences* 45.12 (2003), 2043–2060. DOI: https://doi.org/10.1016/j.ijmecsci.2003.12.008.

[8] Y. Vetyukov et al. Mixed Eulerian—Lagrangian description in materials processing: deformation of a metal sheet in a rolling mill. *International Journal for Numerical Methods in Engineering* 109.10 (2017), 1371–1390. DOI: https://doi.org/10.1002/nme.5314.

[9] V. Longva and S. Sævik. A Lagrangian–Eulerian formulation for reeling analysis of history-dependent multilayered beams. *Computers & Structures* 146 (2015), 44–58. DOI: https://doi.org/10.1016/j.compstruc.2014.09.002.

[10] V. Longva and S. Sævik. On prediction of torque in flexible pipe reeling operations using a Lagrangian–Eulerian FE framework. *Marine Structures* 46 (2016), 229–254. DOI: https://doi.org/10.1016/j.marstruc.2016.01.004.

[11] H. Zhang et al. An efficient multibody dynamic model of arresting cable systems based on ALE formulation. *Mechanism and Machine Theory* 151 (2020), 103892. DOI: https://doi.org/10.1016/j.mechmachtheory.2020.103892.

[12] V. Eliseev and Y. Vetyukov. Effects of deformation in the dynamics of belt drive. *Acta Mechanica* 223.8 (2012), 1657–1667. DOI: 10.1007/s00707-012-0675-3.

[13] Y. Vetyukov, P. G. Gruber and M. Krommer. Nonlinear model of an axially moving plate in a mixed Eulerian–Lagrangian framework. *Acta Mechanica* 227.10 (2016), 2831–2842. DOI: 10.1007/s00707-016-1651-0.

[14] Y. Vetyukov et al. Transient modelling of flexible belt drive dynamics using the equations of a deformable string with discontinuities. *Mathematical and Computer Modelling of Dynamical Systems* 23.1 (2017), 40–54. DOI: 10.1080/13873954.2016.1232281.

[15] E. Oborin, Y. Vetyukov and I. Steinbrecher. Eulerian description of non-stationary motion of an idealized belt-pulley system with dry friction. *International Journal of Solids and Structures* 147 (2018), 40–51. DOI: https://doi.org/10.1016/j.ijsolstr.2018.04.007.

[16] Y. Vetyukov. Non-material finite element modelling of large vibrations of axially moving strings and beams. *Journal of Sound and Vibration* 414 (2018), 299–317. DOI: https://doi.org/10.1016/j.jsv.2017.11.010.

[17] H. Askes, E. Kuhl and P. Steinmann. An ALE formulation based on spatial and material settings of continuum mechanics. Part 2: Classification and applications. *Computer Methods in Applied Mechanics and Engineering* 193.39 (2004), 4223–4245. DOI: https://doi.org/10.1016/j.cma.2003.09.031.

[18] L. Foucard et al. A coupled Eulerian–Lagrangian extended finite element formulation for simulating large deformations in hyperelastic media with moving free boundaries. *Computer Methods in Applied Mechanics and Engineering* 283 (2015), 280–302. DOI: https://doi.org/10.1016/j.cma.2014.09.016.

[19] A. Pechstein and J. Gerstmayr. A Lagrange–Eulerian formulation of an axially moving beam based on the absolute nodal coordinate formulation. *Multibody System Dynamics* 30.3 (2013), 343–358. DOI: 10.1007/s11044-013-9350-2.

[20] J. L. Escalona, G. Orzechowski and A. M. Mikkola. Flexible multibody modeling of reeving systems including transverse vibrations. *Multibody System Dynamics* 44.2 (2018), 107–133. DOI: 10.1007/s11044-018-9619-6.

[21] E. Berger. Friction modeling for dynamic system simulation. *Applied Mechanics Reviews* 55.6 (2002), 535–577. DOI: 10.1115/1.1501080.

[22] V. Yastrebov. Numerical Methods in Contact Mechanics. John Wiley & Sons, Ltd, 2013, 392. DOI: 10.1002/9781118647974.

[23] J. Simo and T. Laursen. An augmented Lagrangian treatment of contact problems involving friction. *Computers & Structures* 42.1 (1992), 97–116. DOI: https://doi.org/10.1016/0045-7949(92)90540-G.

[24] L. Kong and R. G. Parker. Steady Mechanics of Belt-Pulley Systems. *Journal of Applied Mechanics* 72.1 (2005), 25–34. DOI: 10.1115/1.1827251.

[25] A. K. Belyaev et al. Contact of two equal rigid pulleys with a belt modelled as Cosserat nonlinear elastic rod. *Acta Mechanica* 228.12 (2017), 4425–4434. DOI: 10.1007/s00707-017-1942-0.

[26] M. J. Leamy and T. M. Wasfy. Transient and Steady-State Dynamic Finite Element Modeling of Belt-Drives. *Journal of Dynamic Systems, Measurement, and Control* 124.4 (2002), 575–581. DOI: 10.1115/1.1513793.

[27] K. Dufva et al. Nonlinear dynamics of three-dimensional belt drives using the finite-element method. *Nonlinear Dynamics* 48.4 (2007), 449–466. DOI: 10.1007/s11071-006-9098-9.

[28] R. A. Sauer, R. Ghaffari and A. Gupta. The multiplicative deformation split for shells with application to growth, chemical swelling, thermoelasticity, viscoelasticity and elastoplasticity. *International Journal of Solids and Structures* 174-175 (2019), 53–68. DOI: https://doi.org/10.1016/j.ijsolstr.2019.06.002.

[29] E. Hansy-Staudigl and M. Krommer. Electrostrictive polymer plates as electro-elastic material surfaces: Modeling, analysis, and simulation. *Journal of Intelligent Material Systems and Structures* 32.3 (2021), 296–316. DOI: 10.1177/1045389X20935640.

[30] D. G. Alciatore and A. E. Traver. Multipulley Belt Drive Mechanics: Creep Theory vs Shear Theory. *Journal of Mechanical Design* 117.4 (1995), 506–511. DOI: 10.1115/1.2826711.

[31] F. Frendo and F. Bucchi. "Brush model" for the analysis of flat belt transmissions in steady-state conditions. *Mechanism and Machine Theory* 143 (2020), 1036–53. DOI: https://doi.org/10.1016/j.mechmachtheory.2019.103653.

[32] V. Eliseev. The non-linear dynamics of elastic rods. *Journal of Applied Mathematics and Mechanics* 52.4 (1988), 493–498.

[33] S. S. Antman. Nonlinear problems of elasticity. Applied mathematical sciences. New York: Springer, 1995.

[34] O. M. O'Reilly. Modeling Nonlinear Problems in the Mechanics of Strings and Rods: The Role of the Balance Laws. Interaction of Mechanics and Mathematics. Cham: Springer International Publishing, 2017.

[35] Y. Vetyukov. Nonlinear Mechanics of Thin-Walled Structures. Asymptotics, Direct Approach and Numerical Analysis. Foundations of Engineering Mechanics. Vienna: Springer, 2014, 272.

[36] F. Essenburg. On the Significance of the Inclusion of the Effect of Transverse Normal Strain in Problems Involving Beams With Surface Constraints. *Journal of Applied Mechanics* 42.1 (1975), 127–132. DOI: 10.1115/1.3423502.

[37] P. Naghdi and M. Rubin. On the significance of normal cross-sectional extension in beam theory with application to contact problems. *International Journal of Solids and Structures* 25.3 (1989), 249–265. DOI: https://doi.org/10.1016/0020-7683(89)90047-4.

[38] V. V. Eliseev and Y. M. Vetyukov. Finite deformation of thin shells in the context of analytical mechanics of material surfaces. *Acta Mechanica* 209.1 (2009), 43–57. DOI: 10.1007/s00707-009-0154-7.

[39] V. Berdichevskii. Variational-asymptotic method of constructing a theory of shells: PMM vol. 43, no.4, 1979, pp. 664–687. *Journal of Applied Mathematics and Mechanics* 43.4 (1979), 711–736. DOI: https://doi.org/10.1016/0021-8928(79)90157-6.

[40] T. R. Nordenholz and O. M. O'Reilly. On Kinematical Conditions for Steady Motions of Strings and Rods. *Journal of Applied Mechanics* 62.3 (1995), 820–822. DOI: 10.1115/1.2897023.

[41] E. Kocbay and Y. Vetyukov. Stress resultant plasticity for plate bending in the context of roll forming of sheet metal. *International Journal for Numerical Methods in Engineering* (2021). DOI: https://doi.org/10.1002/nme.6760.

[42] P. Bussetta, D. Marceau and J. Ponthot. The adapted augmented Lagrangian method: a new method for the resolution of the mechanical frictional contact problem. *Computational Mechanics* 49 (2012), 259–275. DOI: 10.1007/s00466-011-0644-z.

[43] J. Scheidl and Y. Vetyukov. Coulomb dry friction contact in a non-material shell finite element model for axially moving endless steel belts. *PAMM* 19.1 (2019), e201900260. DOI: https://doi.org/10.1002/pamm.201900260.

[44] M. Dauge and I. Gruais. Edge layers in thin elastic plates. *Computer Methods in Applied Mechanics and Engineering* 157.3 (1998), 335–347. DOI: https://doi.org/10.1016/S0045-7825(97)00244-2.

[45] Y. Vetyukov, A. Kuzin and M. Krommer. Asymptotic splitting in the three-dimensional problem of elasticity for non-homogeneous piezoelectric plates. *International Journal of Solids and Structures* 48.1 (2011), 12–23. DOI: https://doi.org/10.1016/j.ijsolstr.2010.09.001.

[46] A. Gasmi et al. Closed-form solution of a shear deformable, extensional ring in contact between two rigid surfaces. *International Journal of Solids and Structures* 48.5 (2011), 843–853. DOI: https://doi.org/10.1016/j.ijsolstr.2010.11.018.

[47] A. K. Belyaev et al. Static contact of belt and pulleys with account for shear and gravity. *Journal of Physics: Conference Series* 1048 (2018), 012002. DOI: 10.1088/1742-6596/1048/1/012002.

[48] S. Stupkiewicz and Z. Mróz. Elastic beam on a rigid frictional foundation under monotonic and cyclic loading. *International Journal of Solids and Structures* 31.24 (1994), 3419–3442. DOI: https://doi.org/10.1016/0020-7683(94)90024-8.

[49] L. Nikitin et al. On the frictional behaviour of thermally loaded beams resting on a plane. *International Journal of Mechanical Sciences* 38.11 (1996), 1219–1229. DOI: https://doi.org/10.1016/0020-7403(96)00009-4.

[50] Y. Vetyukov. Endless elastic beam travelling on a moving rough surface with zones of stick and sliding. *Nonlinear Dynamics* 104.4 (2021), 3309–3321. DOI: 10.1007/s11071-021-06523-y.

[51] A. K. Belyaev et al. Dynamics of Contour Motion of Belt Drive by Means of Nonlinear Rod Approach. *Dynamics and Control of Advanced Structures and Machines: Contributions from the 3rd International Workshop, Perm, Russia*. Ed. by V. P. Matveenko et al. Cham: Springer International Publishing, 2019, 21–29. DOI: 10.1007/978-3-319-90884-7_3.

[52] E. Oborin and Y. Vetyukov. Steady state motion of a shear deformable beam in contact with a traveling surface. *Acta Mechanica* 230.11 (2019), 4021–4033. DOI: 10.1007/s00707-019-02476-x.

[53] E. Oborin. Belt–pulley interaction: role of the action line of friction forces. *Acta Mechanica* 231.9 (2020), 3979–3987. DOI: 10.1007/s00707-020-02724-5.

[54] J. Wickert. Non-linear vibration of a traveling tensioned beam. *International Journal of Non-Linear Mechanics* 27.3 (1992), 503–517. DOI: https://doi.org/10.1016/0020-7462(92)90016-Z.

[55] H. Irschik and H. J. Holl. The equations of Lagrange written for a non-material volume. *Acta Mechanica* 153.3 (2002), 231–248. DOI: 10.1007/BF01177454.

[56] A. Steinboeck, M. Saxinger and A. Kugi. Hamilton's Principle for Material and Nonmaterial Control Volumes Using Lagrangian and Eulerian Description of Motion. *Applied Mechanics Reviews* 71.1 (2019), 010802. DOI: https://doi.org/10.1115/1.4042434.

[57] F. Bogner, R. Fox and L. Schmit. The generation of interelement compatible stiffness and mass matrices by the use of interpolation formulae. *Proc. 1st Conf. Matrix Methods in Structural Mechanics*. Vol. AFFDL-TR-66-80. Wright Patterson Air force Base, Ohio, 1966, 397–443.

[58] Y. Vetyukov. Finite element modeling of Kirchhoff-Love shells as smooth material surfaces. *ZAMM - Journal of Applied Mathematics and Mechanics / Zeitschrift für Angewandte Mathematik und Mechanik* 94 (2014), 150–163. DOI: https://doi.org/10.1002/zamm.201200179.

[59] O. Zienkiewicz, R. Taylor and J. Zhu. Chapter 3 - Weak Forms and Finite Element Approximation: 1-D Problems. *The Finite Element Method: its Basis and Fundamentals*. Ed. by O. Zienkiewicz, R. Taylor and J. Zhu. Seventh Edition. Oxford: Butterworth-Heinemann, 2013, 47–92. DOI: https://doi.org/10.1016/B978-1-85617-633-0.00003-4.

[60] M. Ambati, J. Kiendl and L. De Lorenzis. Isogeometric Kirchhoff–Love shell formulation for elasto-plasticity. *Computer Methods in Applied Mechanics and Engineering* 340 (2018), 320–339. DOI: https://doi.org/10.1016/j.cma.2018.05.023.

[61] G. Radenković, A. Borković and B. Marussig. Nonlinear static isogeometric analysis of arbitrarily curved Kirchhoff-Love shells. *International Journal of Mechanical Sciences* 192 (2021), 106143. DOI: https://doi.org/10.1016/j.ijmecsci.2020.106143.

[62] K.-J. Bathe, A. Iosilevich and D. Chapelle. An evaluation of the MITC shell elements. *Computers & Structures* 75.1 (2000), 1–30. DOI: https://doi.org/10.1016/S0045-7949(99)00214-X.

[63] J. Scheidl et al. Mixed Eulerian–Lagrangian description in the statics of a flexible belt with tension and bending hanging on two pulleys. *PAMM* 18.1 (2018), e201800060. DOI: https://doi.org/10.1002/pamm.201800060.

Paper A

Flexible belt hanging on two pulleys: Contact problem at non-material kinematic description

TU Wien: Yury Vetyukov, Jakob Scheidl, Michael Krommer, Christian Schmidrathner
JKU Linz: Evgenii Oborin
International Journal of Solids and Structures 168 (2019), 183–193
https://doi.org/10.1016/j.ijsolstr.2019.03.034

Keywords: Belt drive mechanics, Mixed Eulerian–Lagrangian description, Finite element analysis, Contact problem, Kirchhoff rod theory

Abstract: We propose a non-material finite element scheme for modelling large deformations of a closed flexible rod supported by two rigid pulleys in the field of gravity. The mixed Eulerian–Lagrangian kinematic description of circumferential and transverse displacements is beneficial for simulations of moving belt drives. The necessary C^1 inter-element continuity in a compound coordinate system with Cartesian and polar domains requires a nonlinear finite element approximation. The theoretically predicted singular reaction force distribution prevents us from using the technique of Lagrange multipliers for normal contact. A novel semi-analytical solution of the static problem based on the integration of the equations of the nonlinear theory of rods in the free spans as well as in the segments of contact with pulleys is presented for the sake of validation. We demonstrate the mutual convergence of simulation results for a benchmark problem and additionally justify them by comparison against conventional Lagrangian finite element solutions.

References of Paper A

[1] S. S. Antman. The Theory of Rods. *Linear Theories of Elasticity and Thermoelasticity: Linear and Nonlinear Theories of Rods, Plates, and Shells*. Ed. by C. Truesdell. Berlin, Heidelberg: Springer Berlin Heidelberg, 1973, 641–703. DOI: 10.1007/978-3-662-39776-3_6.

[2] U. Ascher and R. D. Russell. Reformulation of boundary value problems into "standard" form. *SIAM Review* 23.2 (1981), 238–254. DOI: 10.1137/1023039.

[3] M. Batista. Large deflections of an elastic rod in contact with a flat wall. *International Journal of Solids and Structures* 115-116 (2017), 53–60. DOI: https://doi.org/10.1016/j.ijsolstr.2017.02.030.

[4] S. E. Bechtel et al. The Stretching and Slipping of Belts and Fibers on Pulleys. *Journal of Applied Mechanics* 67.1 (1999), 197–206. DOI: 10.1115/1.321164.

[5] A. Belyaev et al. Contact of two equal rigid pulleys with a belt modelled as Cosserat nonlinear elastic rod. *Acta Mechanica* 228.12 (2017), 4425–4434. DOI: 10.1007/s00707-017-1942-0.

[6] A. K. Belyaev et al. Static contact of belt and pulleys with account for shear and gravity. *Journal of Physics: Conference Series* 1048 (2018), 012002. DOI: 10.1088/1742-6596/1048/1/012002.

[7] A. K. Belyaev et al. On static contact of belt and different pulleys. *IOP Conference Series: Materials Science and Engineering* 208 (2017), 012004. DOI: 10.1088/1757-899x/208/1/012004.

[8] J.-S. Chen and L.-Y. Hua. Effects of clamping misalignments on the line-contact deformation of a constrained elastica. *International Journal of Non-Linear Mechanics* 99 (2018), 288–294. DOI: https://doi.org/10.1016/j.ijnonlinmec.2017.12.009.

[9] L.-Q. Chen. Analysis and Control of Transverse Vibrations of Axially Moving Strings. *Applied Mechanics Reviews* 58.2 (2005), 91–116. DOI: 10.1115/1.1849169.

[10] V. Denoël. Advantages of a semi-analytical approach for the analysis of an evolving structure with contacts. *Communications in Numerical Methods in Engineering* 24 (2007), 1667–1683. DOI: 10.1002/cnm.1059.

[11] V. Denoël and E. Detournay. Eulerian formulation of constrained elastica. *International Journal of Solids and Structures* 48.3 (2011), 625–636. DOI: https://doi.org/10.1016/j.ijsolstr.2010.10.027.

[12] K. Dufva et al. Nonlinear dynamics of three-dimensional belt drives using the finite-element method. *Nonlinear Dynamics* 48.4 (2007), 449–466. DOI: 10.1007/s11071-006-9098-9.

[13] V. Eliseev. Mechanics of deformable solid bodies. St. Petersburg: St. Petersburg State Polytechnical University Publishing House, 2006.

[14] V. Eliseev and Y. Vetyukov. Effects of deformation in the dynamics of belt drive. *Acta Mechanica* 223.8 (2012), 1657–1667. DOI: 10.1007/s00707-012-0675-3.

[15] V. V. Yeliseev and T. V. Zinovieva. Nonlinear-elastic strain of underwater pipeline in laying process. *Computational Continuum Mechanics* 5.1 (2012), 70–78. DOI: https://doi.org/10.7242/1999-6691/2012.5.1.9.

[16] J. L. Escalona, G. Orzechowski and A. M. Mikkola. Flexible multibody modeling of reeving systems including transverse vibrations. *Multibody System Dynamics* 44.2 (2018), 107–133. DOI: 10.1007/s11044-018-9619-6.

[17] A. Gasmi et al. Closed-form solution of a shear deformable, extensional ring in contact between two rigid surfaces. *International Journal of Solids and Structures* 48.5 (2011), 843–853. DOI: https://doi.org/10.1016/j.ijsolstr.2010.11.018.

[18] V. Goss and R. Chaouki. Loading paths for an elastic rod in contact with a flat inclined surface. *International Journal of Solids and Structures* 88-89 (2016), 274–282. DOI: https://doi.org/10.1016/j.ijsolstr.2016.02.042.

[19] P. G. Gruber et al. A novel director-based Bernoulli–Euler beam finite element in absolute nodal coordinate formulation free of geometric singularities. *Mechanical Sciences* 4.2 (2013), 279–289. DOI: 10.5194/ms-4-279-2013.

[20] D. Hong and G. Ren. A modeling of sliding joint on one-dimensional flexible medium. *Multibody System Dynamics* 26.1 (2011), 91–106. DOI: 10.1007/s11044-010-9242-7.

[21] A. Huynen, E. Detournay and V. Denoël. Eulerian formulation of elastic rods. *Proceedings of the Royal Society A: Mathematical, Physical and Engineering Sciences* 472.2190 (2016), 20150547. DOI: 10.1098/rspa.2015.0547.

[22] S. Kaczmarczyk and S. Mirhadizadeh. Quasi-stationary mechanics of elastic continua with bending stiffness wrapping on a pulley system. *Journal of Physics: Conference Series* 721 (2016), 012011. DOI: 10.1088/1742-6596/721/1/012011.

[23] J. Kierzenka and L. F. Shampine. A BVP Solver Based on Residual Control and the Maltab PSE. *ACM Trans. Math. Softw.* 27.3 (2001), 299–316. DOI: 10.1145/502800.502801.

[24] J.-P. Liu, Z.-B. Cheng and G.-X. Ren. An Arbitrary Lagrangian–Eulerian formulation of a geometrically exact Timoshenko beam running through a tube. *Acta Mechanica* 229.8 (2018), 3161–3188. DOI: 10.1007/s00707-018-2161-z.

[25] T. Morimoto and H. Iizuka. Rolling contact between a rubber ring and rigid cylinders: Mechanics of rubber belts. *International Journal of Mechanical Sciences* 54.1 (2012), 234–240. DOI: https://doi.org/10.1016/j.ijmecsci.2011.11.001.

[26] E. Oborin, Y. Vetyukov and I. Steinbrecher. Eulerian description of non-stationary motion of an idealized belt-pulley system with dry friction. *International Journal of Solids and Structures* 147 (2018), 40–51. DOI: https://doi.org/10.1016/j.ijsolstr.2018.04.007.

[27] M. B. Rubin. An Exact Solution for Steady Motion of an Extensible Belt in Multipulley Belt Drive Systems. *Journal of Mechanical Design* 122.3 (2000), 311–316. DOI: 10.1115/1.1288404.

[28] J. Scheidl et al. Mixed Eulerian–Lagrangian description in the statics of a flexible belt with tension and bending hanging on two pulleys. *PAMM* 18.1 (2018), e201800060. DOI: https://doi.org/10.1002/pamm.201800060.

[29] J. Simo and T. Laursen. An augmented Lagrangian treatment of contact problems involving friction. *Computers & Structures* 42.1 (1992), 97–116. DOI: https://doi.org/10.1016/0045-7949(92)90540-G.

[30] I. Steinbrecher, A. Humer and L. Vu-Quoc. On the numerical modeling of sliding beams: A comparison of different approaches. *Journal of Sound and Vibration* 408 (2017), 270–290. DOI: https://doi.org/10.1016/j.jsv.2017.07.010.

[31] S. Timoshenko and J. Gere. Theory of Elastic Stability. 2nd. New-York: McGraw-Hill, 1961. Chap. 5.

[32] L. N. Trefethen, A. Birkisson and T. A. Driscoll. Exploring ODEs. Vol. 157. SIAM, 2017.

[33] Y. Vetyukov. Hybrid asymptotic-direct approach to the problem of finite vibrations of a curved layered strip. *Acta Mechanica* 223.2 (2012), 371–385. DOI: 10.1007/s00707-011-0562-3.

[34] Y. Vetyukov. Non-material finite element modelling of large vibrations of axially moving strings and beams. *Journal of Sound and Vibration* 414 (2018), 299–317. DOI: https://doi.org/10.1016/j.jsv.2017.11.010.

[35] Y. Vetyukov, P. G. Gruber and M. Krommer. Nonlinear model of an axially moving plate in a mixed Eulerian–Lagrangian framework. *Acta Mechanica* 227.10 (2016), 2831–2842. DOI: 10.1007/s00707-016-1651-0.

[36] Y. Vetyukov et al. Mixed Eulerian–Lagrangian description in materials processing: deformation of a metal sheet in a rolling mill. *International Journal for Numerical Methods in Engineering* 109.10 (2017), 1371–1390. DOI: https://doi.org/10.1002/nme.5314.

[37] Y. Vetyukov et al. Transient modelling of flexible belt drive dynamics using the equations of a deformable string with discontinuities. *Mathematical and Computer Modelling of Dynamical Systems* 23.1 (2017), 40–54. DOI: 10.1080/13873954.2016.1232281.

Paper B

Motion of a friction belt drive at mixed kinematic description

TU Wien: Jakob Scheidl
International Journal of Solids and Structures 200–201 (2020), 158–169
https://doi.org/10.1016/j.ijsolstr.2020.05.001

Keywords: Belt drive mechanics, Mixed Eulerian Lagrangian kinematics, Structural finite elements, Rod theory, Dry friction contact

Abstract: We revisit the planar problem of a two-pulley belt drive and extend an existing mixed Eulerian–Lagrangian finite element framework to simulate the quasistatic, non-stationary motion. The mixed kinematic description proves beneficial in the consistent modelling of Coulomb dry friction in the contact domains between deformable belt and rigid pulleys. In particular, the method of augmented Lagrangian multipliers is adopted for contact treatment, which relies on the penalty regularisation to iteratively update estimates for the contact tractions. In addition, a semi-analytic strategy to compute steady state solutions is presented. Contrary to similar studies available in the literature, it accounts for gravity, which changes the size of the contact regions and induces large transverse deflections. The comparative study demonstrates correspondence of steady state solutions obtained with both approaches. Results regarding the time evolution of the contact state demonstrate the potential of the proposed finite element scheme.

References of Paper B

[1] S. E. Bechtel et al. The Stretching and Slipping of Belts and Fibers on Pulleys. *Journal of Applied Mechanics* 67.1 (1999), 197–206. DOI: 10.1115/1.321164.

[2] A. K. Belyaev et al. Contact of two equal rigid pulleys with a belt modelled as Cosserat nonlinear elastic rod. *Acta Mechanica* 228.12 (2017), 4425–4434. DOI: 10.1007/s00707-017-1942-0.

[3] A. K. Belyaev et al. Static contact of belt and pulleys with account for shear and gravity. *Journal of Physics: Conference Series* 1048 (2018), 012002. DOI: 10.1088/1742-6596/1048/1/012002.

[4] K. Dufva et al. Nonlinear dynamics of three-dimensional belt drives using the finite-element method. *Nonlinear Dynamics* 48.4 (2007), 449–466. DOI: 10.1007/s11071-006-9098-9.

[5] V. Eliseev and Y. Vetyukov. Effects of deformation in the dynamics of belt drive. *Acta Mechanica* 223.8 (2012), 1657–1667. DOI: 10.1007/s00707-012-0675-3.

[6] M. H. Ghayesh, H. A. Kafiabad and T. Reid. Sub- and super-critical nonlinear dynamics of a harmonically excited axially moving beam. *International Journal of Solids and Structures* 49.1 (2012), 227–243. DOI: https://doi.org/10.1016/j.ijsolstr.2011.10.007.

[7] J. Hoffman, J. Jansson and M. Stöckli. Unified continuum modeling of fluid-structure interaction. *Mathematical Models and Methods in Applied Sciences* 21.03 (2011), 491–513. DOI: 10.1142/S021820251100512X.

[8] H. Irschik and J. Gerstmayr. A continuum mechanics based derivation of Reissner's large-displacement finite-strain beam theory: the case of plane deformations of originally straight Bernoulli–Euler beams. *Acta Mechanica* 206.1 (2009), 1–21. DOI: 10.1007/s00707-008-0085-8.

[9] D. Kim, M. Leamy and A. Ferri. Dynamic Modeling of Flat Belt Drives Using the Elastic-Perfectly-Plastic Friction Law. *Proceedings of the ASME Design Engineering Technical Conference*. Vol. Volume 4: 7th International Conference on Multibody Systems, Nonlinear Dynamics, and Control, Parts A, B and C. International Design Engineering Technical Conferences and Computers and Information in Engineering Conference. 2009, 483–491. DOI: 10.1115/DETC2009-87296.

[10] L. Kong and R. G. Parker. Steady Mechanics of Belt-Pulley Systems. *Journal of Applied Mechanics* 72.1 (2005), 25–34. DOI: 10.1115/1.1827251.

[11] M. J. Leamy. On a Perturbation Method for the Analysis of Unsteady Belt-Drive Operation. *Journal of Applied Mechanics* 72.4 (2004), 570–580. DOI: 10.1115/1.1940660.

[12] M. J. Leamy and T. M. Wasfy. Transient and Steady-State Dynamic Finite Element Modeling of Belt-Drives. *Journal of Dynamic Systems, Measurement, and Control* 124.4 (2002), 575–581. DOI: 10.1115/1.1513793.

[13] A. R. Mojdehi, D. P. Holmes and D. A. Dillard. Friction of extensible strips: An extended shear lag model with experimental evaluation. *International Journal of Solids and Structures* 124 (2017), 125–134. DOI: https://doi.org/10.1016/j.ijsolstr.2017.06.021.

[14] T. R. Nordenholz and O. M. O'Reilly. On Kinematical Conditions for Steady Motions of Strings and Rods. *Journal of Applied Mechanics* 62.3 (1995), 820–822. DOI: 10.1115/1.2897023.

[15] E. Oborin, Y. Vetyukov and I. Steinbrecher. Eulerian description of non-stationary motion of an idealized belt-pulley system with dry friction. *International Journal of Solids and Structures* 147 (2018), 40–51. DOI: https://doi.org/10.1016/j.ijsolstr.2018.04.007.

[16] A. Pechstein and J. Gerstmayr. A Lagrange–Eulerian formulation of an axially moving beam based on the absolute nodal coordinate formulation. *Multibody System Dynamics* 30.3 (2013), 343–358. DOI: 10.1007/s11044-013-9350-2.

[17] B. Radi, O. Baba and J.-C. Gelin. Treatment of the frictional contact via a Lagrangian formulation. *Mathematical and Computer Modelling* 28.4 (1998), 407–412. DOI: https://doi.org/10.1016/S0895-7177(98)00130-7.

[18] M. B. Rubin. An Exact Solution for Steady Motion of an Extensible Belt in Multipulley Belt Drive Systems. *Journal of Mechanical Design* 122.3 (2000), 311–316. DOI: 10.1115/1.1288404.

[19] J. Simo and T. Laursen. An augmented Lagrangian treatment of contact problems involving friction. *Computers & Structures* 42.1 (1992), 97–116. DOI: https://doi.org/10.1016/0045-7949(92)90540-G.

[20] I. Steinbrecher, A. Humer and L. Vu-Quoc. On the numerical modeling of sliding beams: A comparison of different approaches. *Journal of Sound and Vibration* 408 (2017), 270–290. DOI: https://doi.org/10.1016/j.jsv.2017.07.010.

[21] J. Synka and A. Kainz. A novel mixed Eulerian–Lagrangian finite-element method for steady-state hot rolling processes. *International Journal of Mechanical Sciences* 45.12 (2003), 2043–2060. DOI: https://doi.org/10.1016/j.ijmecsci.2003.12.008.

[22] A. Ulsoy and C. Mote. Vibration of Wide Band Saw Blades. *ASME Journal of Engineering for Industry* 104 (1982), 71–78. DOI: 10.1115/1.3185801.

[23] Y. Vetyukov. Non-material finite element modelling of large vibrations of axially moving strings and beams. *Journal of Sound and Vibration* 414 (2018), 299–317. DOI: https://doi.org/10.1016/j.jsv.2017.11.010.

[24] Y. Vetyukov et al. Mixed Eulerian—Lagrangian description in materials processing: deformation of a metal sheet in a rolling mill. *International Journal for Numerical Methods in Engineering* 109.10 (2017), 1371–1390. DOI: 10.1002/nme.5314.

[25] Y. Vetyukov et al. Transient modelling of flexible belt drive dynamics using the equations of a deformable string with discontinuities. *Mathematical and Computer Modelling of Dynamical Systems* 23.1 (2017), 40–54. DOI: 10.1080/13873954.2016.1232281.

[26] Y. Vetyukov et al. Flexible belt hanging on two pulleys: Contact problem at non-material kinematic description. *International Journal of Solids and Structures* 168 (2019), 183–193. DOI: https://doi.org/10.1016/j.ijsolstr.2019.03.034.

[27] J. Wickert. Non-linear vibration of a traveling tensioned beam. *International Journal of Non-Linear Mechanics* 27.3 (1992), 503–517. DOI: https://doi.org/10.1016/0020-7462(92)90016-Z.

[28] V. Yastrebov. Numerical Methods in Contact Mechanics. John Wiley & Sons, Ltd, 2013, 392. DOI: 10.1002/9781118647974.

Paper C

Steady motion of a belt in frictional contact with a rotating pulley

TU Wien: Jakob Scheidl, Yury Vetyukov
Dynamics and Control of Advanced Structures and Machines (2021)
https://doi.org/10.1007/978-3-030-79325-8_18

Abstract: The steady state motion of belt drives is studied extensively in the literature. While traditional models rely on the theory of an extensible string, we aim to take bending effects into account. In this regard, it is well known that concentrated contact forces at the points of first and last contact with a pulley arise if shear deformations are restricted. To circumvent this issue, we utilize a shear deformable, Cosserat theory of rods. In particular, we study the contour motion of a belt that is transported over a single, rigid pulley with zones of stick, sliding friction and no contact. The Coulomb friction law governs the contact between the belt and the pulley. We present a novel finite element model that allows to obtain the steady state solution directly. Furthermore, we deduce the corresponding closed boundary value problem and integrate it numerically. Results obtained for a particular parameter set demonstrate correspondence of the two approaches.

References of Paper C

[1] A. K. Belyaev et al. Dynamics of Contour Motion of Belt Drive by Means of Nonlinear Rod Approach. *Dynamics and Control of Advanced Structures and Machines: Contributions from the 3rd International Workshop, Perm, Russia*. Ed. by V. P. Matveenko et al. Cham: Springer International Publishing, 2019, 21–29. DOI: 10.1007/978-3-319-90884-7_3.

[2] E. Oborin and Y. Vetyukov. Steady state motion of a shear deformable beam in contact with a traveling surface. *Acta Mechanica* 230.11 (2019), 4021–4033. DOI: 10.1007/s00707-019-02476-x.

[3] J. Simo and T. Laursen. An augmented Lagrangian treatment of contact problems involving friction. *Computers & Structures* 42.1 (1992), 97–116. DOI: https://doi.org/10.1016/0045-7949(92)90540-G.

[4] Y. Vetyukov et al. Flexible belt hanging on two pulleys: Contact problem at non-material kinematic description. *International Journal of Solids and Structures* 168 (2019), 183–193. DOI: https://doi.org/10.1016/j.ijsolstr.2019.03.034.

Paper D

Steady motion of a slack belt drive: Dynamics of a beam in frictional contact with rotating pulleys

TU Wien: Jakob Scheidl, Yury Vetyukov
ASME Journal of Applied Mechanics 87.12 (2020), 121011
https://doi.org/10.1115/1.4048317

Keywords: computational mechanics, dynamics, elasticity, structures

Abstract: We seek the steady state motion of a slack two-pulley belt drive with the belt modelled as an elastic, shear-deformable rod. Dynamic effects and gravity induce significant transverse deflections due to the low pre-tension. In analogy to belt-creep theory, it is assumed that each contact region between the belt and one of the pulleys consists of a single sticking and a single sliding zone. Based on the governing equations of the rod theory, we for the first time derive the corresponding boundary value problem and integrate it numerically. Furthermore, a novel mixed Eulerian-Lagrangian finite element scheme is developed that iteratively seeks the steady state solution. Finite element solutions are validated against semi-analytic results obtained by numerical integration of the boundary value problem. Parameter studies are conducted to examine solution dependence on the stiffness coefficients and the belt pre-tension.

References of Paper D

[1] M. B. Rubin. An Exact Solution for Steady Motion of an Extensible Belt in Multipulley Belt Drive Systems. *Journal of Mechanical Design* 122.3 (2000), 311–316. DOI: 10.1115/1.1288404.

[2] F. Frendo and F. Bucchi. "Brush model" for the analysis of flat belt transmissions in steady-state conditions. *Mechanism and Machine Theory* 143 (2020), 1036–53. DOI: https://doi.org/10.1016/j.mechmachtheory.2019.103653.

[3] D. G. Alciatore and A. E. Traver. Multipulley Belt Drive Mechanics: Creep Theory vs Shear Theory. *Journal of Mechanical Design* 117.4 (1995), 506–511. DOI: 10.1115/1.2826711.

[4] Y. Wu, M. J. Leamy and M. Varenberg. Belt-Drive Mechanics: Friction in the Absence of Sliding. *Journal of Applied Mechanics* 86.10 (2019). DOI: 10.1115/1.4044019.

[5] S. E. Bechtel et al. The Stretching and Slipping of Belts and Fibers on Pulleys. *Journal of Applied Mechanics* 67.1 (1999), 197–206. DOI: 10.1115/1.321164.

[6] L. Kong and R. G. Parker. Steady Mechanics of Belt-Pulley Systems. *Journal of Applied Mechanics* 72.1 (2005), 25–34. DOI: 10.1115/1.1827251.

[7] A. K. Belyaev et al. Contact of two equal rigid pulleys with a belt modelled as Cosserat nonlinear elastic rod. *Acta Mechanica* 228.12 (2017), 4425–4434. DOI: 10.1007/s00707-017-1942-0.

[8] M. J. Leamy. On a Perturbation Method for the Analysis of Unsteady Belt-Drive Operation. *Journal of Applied Mechanics* 72.4 (2004), 570–580. DOI: 10.1115/1.1940660.

[9] Y. Vetyukov et al. Transient modelling of flexible belt drive dynamics using the equations of a deformable string with discontinuities. *Mathematical and Computer Modelling of Dynamical Systems* 23.1 (2017), 40–54. DOI: 10.1080/13873954.2016.1232281.

[10] E. Oborin, Y. Vetyukov and I. Steinbrecher. Eulerian description of non-stationary motion of an idealized belt-pulley system with dry friction. *International Journal of Solids and Structures* 147 (2018), 40–51. DOI: https://doi.org/10.1016/j.ijsolstr.2018.04.007.

[11] K. Dufva et al. Nonlinear dynamics of three-dimensional belt drives using the finite-element method. *Nonlinear Dynamics* 48.4 (2007), 449–466. DOI: 10.1007/s11071-006-9098-9.

[12] M. J. Leamy and T. M. Wasfy. Transient and Steady-State Dynamic Finite Element Modeling of Belt-Drives. *Journal of Dynamic Systems, Measurement, and Control* 124.4 (2002), 575–581. DOI: 10.1115/1.1513793.

[13] Y. Vetyukov. Non-material finite element modelling of large vibrations of axially moving strings and beams. *Journal of Sound and Vibration* 414 (2018), 299–317. DOI: https://doi.org/10.1016/j.jsv.2017.11.010.

[14] J. Scheidl. Motion of a friction belt drive at mixed kinematic description. *International Journal of Solids and Structures* (2020). DOI: https://doi.org/10.1016/j.ijsolstr.2020.05.001.

[15] J. Synka and A. Kainz. A novel mixed Eulerian-–Lagrangian finite-element method for steady-state hot rolling processes. *International Journal of Mechanical Sciences* 45.12 (2003), 2043–2060. DOI: https://doi.org/10.1016/j.ijmecsci.2003.12.008.

[16] Y. Vetyukov et al. Mixed Eulerian—Lagrangian description in materials processing: deformation of a metal sheet in a rolling mill. *International Journal for Numerical Methods in Engineering* 109.10 (2017), 1371–1390. DOI: 10.1002/nme.5314.

[17] V. Longva and S. Sævik. A Lagrangian–Eulerian formulation for reeling analysis of history-dependent multilayered beams. *Computers & Structures* 146 (2015), 44–58. DOI: https://doi.org/10.1016/j.compstruc.2014.09.002.

[18] J. L. Escalona, G. Orzechowski and A. M. Mikkola. Flexible multibody modeling of reeving systems including transverse vibrations. *Multibody System Dynamics* 44.2 (2018), 107–133. DOI: 10.1007/s11044-018-9619-6.

[19] A. E. Green and N. Laws. A General Theory of Rods. *Proceedings of the Royal Society of London. Series A, Mathematical and Physical Sciences* 293.1433 (1966), 145–155.

[20] F. Essenburg. On the Significance of the Inclusion of the Effect of Transverse Normal Strain in Problems Involving Beams With Surface Constraints. *Journal of Applied Mechanics* 42.1 (1975), 127–132. DOI: 10.1115/1.3423502.

[21] P. Naghdi and M. Rubin. On the significance of normal cross-sectional extension in beam theory with application to contact problems. *International Journal of Solids and Structures* 25.3 (1989), 249–265. DOI: https://doi.org/10.1016/0020-7683(89)90047-4.

[22] T. Nordenholz and O. O'Reilly. On steady motions of an elastic rod with application to contact problems. *International Journal of Solids and Structures* 34.9 (1997), 1123–1143. DOI: https://doi.org/10.1016/S0020-7683(96)00054-6.

[23] D. Kim, M. Leamy and A. Ferri. Dynamic Modeling of Flat Belt Drives Using the Elastic-Perfectly-Plastic Friction Law. *Proceedings of the ASME Design Engineering Technical Conference*. Vol. Volume 4: 7th International Conference on Multibody Systems, Nonlinear Dynamics, and Control, Parts A, B and C. International Design Engineering Technical Conferences and Computers and Information in Engineering Conference. 2009, 483–491. DOI: 10.1115/DETC2009-87296.

[24] M. H. Ghayesh, H. A. Kafiabad and T. Reid. Sub- and super-critical nonlinear dynamics of a harmonically excited axially moving beam. *International Journal of Solids and Structures* 49.1 (2012), 227–243. DOI: https://doi.org/10.1016/j.ijsolstr.2011.10.007.

[25] A. Steindl. Oscillations of a visco-elastic belt drive. *PAMM* 17.1 (2017), 381–382. DOI: https://doi.org/10.1002/pamm.201710160.

[26] A. K. Belyaev et al. Dynamics of Contour Motion of Belt Drive by Means of Nonlinear Rod Approach. *Dynamics and Control of Advanced Structures and Machines: Contributions from the 3rd International Workshop, Perm, Russia*. Ed. by V. P. Matveenko et al. Cham: Springer International Publishing, 2019, 21–29. DOI: 10.1007/978-3-319-90884-7_3.

[27] J. Simo and T. Laursen. An augmented Lagrangian treatment of contact problems involving friction. *Computers & Structures* 42.1 (1992), 97–116. DOI: https://doi.org/10.1016/0045-7949(92)90540-G.

[28] V. Yastrebov. Numerical Methods in Contact Mechanics. John Wiley & Sons, Ltd, 2013, 392. DOI: 10.1002/9781118647974.

[29] Y. Vetyukov et al. Flexible belt hanging on two pulleys: Contact problem at non-material kinematic description. *International Journal of Solids and Structures* 168 (2019), 183–193. DOI: https://doi.org/10.1016/j.ijsolstr.2019.03.034.

[30] P. Naghdi and M. Rubin. Constrained theories of rods. *Journal of Elasticity* 14.4 (1984), 343–361. DOI: 10.1007/BF00125605.

[31] J. Scheidl and Y. Vetyukov. Steady motion of a belt in frictional contact with a rotating pulley. *Dynamics and Control of Advanced Structures and Machines*. Ed. by V. P. Matveenko et al. Springer International Publishing, 2021. DOI: https://doi.org/10.1007/978-3-030-79325-8_18.

[32] E. Oborin and Y. Vetyukov. Steady state motion of a shear deformable beam in contact with a traveling surface. *Acta Mechanica* 230.11 (2019), 4021–4033. DOI: 10.1007/s00707-019-02476-x.

[33] E. Oborin. Belt–pulley interaction: role of the action line of friction forces. *Acta Mechanica* 231.9 (2020), 3979–3987. DOI: 10.1007/s00707-020-02724-5.

[34] S. S. Antman. Nonlinear problems of elasticity. Applied mathematical sciences. New York: Springer, 1995.

[35] O. M. O'Reilly. Modeling Nonlinear Problems in the Mechanics of Strings and Rods: The Role of the Balance Laws. Interaction of Mechanics and Mathematics. Cham: Springer International Publishing, 2017.

[36] V. Eliseyev. The non-linear dynamics of elastic rods. *Journal of Applied Mathematics and Mechanics* 52.4 (1988), 493–498. DOI: https://doi.org/10.1016/0021-8928(88)90039-1.

[37] T. R. Nordenholz and O. M. O'Reilly. On Kinematical Conditions for Steady Motions of Strings and Rods. *Journal of Applied Mechanics* 62.3 (1995), 820–822. DOI: 10.1115/1.2897023.

[38] V. Eliseev and Y. Vetyukov. Effects of deformation in the dynamics of belt drive. *Acta Mechanica* 223.8 (2012), 1657–1667. DOI: 10.1007/s00707-012-0675-3.

[39] J. Wickert. Non-linear vibration of a traveling tensioned beam. *International Journal of Non-Linear Mechanics* 27.3 (1992), 503–517. DOI: https://doi.org/10.1016/0020-7462(92)90016-Z.

[40] P. Bussetta, D. Marceau and J. Ponthot. The adapted augmented Lagrangian method: a new method for the resolution of the mechanical frictional contact problem. *Computational Mechanics* 49 (2012), 259–275. DOI: 10.1007/s00466-011-0644-z.

Paper E

Mixed Eulerian–Lagrangian shell model for lateral run-off in a steel belt drive and its experimental validation

TU Wien: Jakob Scheidl, Yury Vetyukov, Christian Schmidrathner
Berndorf Band GmbH: Klemens Schulmeister, Michael Proschek
International Journal of Mechanical Sciences 204 (2021), 106572
https://doi.org/10.1016/j.ijmecsci.2021.106572

Keywords: Mixed Eulerian–Lagrangian description, Kirchhoff shell, Finite element analysis, Belt drive mechanics, Elastic contact, Transient analysis

Abstract: A non-material shell finite element model is developed and applied to the example problem of a slack steel belt moving on two rotating drums. For the first time in the open literature we demonstrate an approach for predicting the time evolution of the lateral run-off velocity of the belt in response to its geometric imperfection and angular drum misalignment. We adopt a novel Eulerian–Lagrangian kinematic description featuring a mixed parametrisation of the configurational space with a Eulerian circumferential coordinate and two Lagrangian coordinates for the transverse and lateral deflections. A nonlinear finite element approximation provides the necessary C^1 inter-element continuity in this compound coordinate system. Using the model of elastic tangential contact, we account for the convective term in the local increments of the relative displacement between the contacting surfaces during the time integration. A thorough convergence study with respect to the mesh and time step sizes justifies the approach. Together with the successful validation against the results of a series of physical experiments, this makes the present contribution an important step towards a model-based controller design.

References of Paper E

[1] C. Mote. Divergence buckling of an edge-loaded axially moving band. *International Journal of Mechanical Sciences* 10.4 (1968), 281–295. DOI: https://doi.org/10.1016/0020-7403(68)90013-1.

[2] G. Spelsberg-Korspeter, O. N. Kirillov and P. Hagedorn. Modeling and Stability Analysis of an Axially Moving Beam With Frictional Contact. *Journal of Applied Mechanics* 75.3 (2008), 031001. DOI: 10.1115/1.2755166.

[3] K. Marynowski and T. Kapitaniak. Dynamics of axially moving continua. *International Journal of Mechanical Sciences* 81 (2014), 26–41. DOI: https://doi.org/10.1016/j.ijmecsci.2014.01.017.

[4] K. Marynowski. Free vibration analysis of an axially moving multiscale composite plate including thermal effect. *International Journal of Mechanical Sciences* 120 (2017), 62–69. DOI: https://doi.org/10.1016/j.ijmecsci.2016.11.013.

[5] M. H. Ghayesh and M. Amabili. Post-buckling bifurcations and stability of high-speed axially moving beams. *International Journal of Mechanical Sciences* 68 (2013), 76–91. DOI: https://doi.org/10.1016/j.ijmecsci.2013.01.001.

[6] Y. Vetyukov. Finite element modeling of Kirchhoff-Love shells as smooth material surfaces. *ZAMM - Journal of Applied Mathematics and Mechanics / Zeitschrift für Angewandte Mathematik und Mechanik* 94 (2014), 150–163. DOI: https://doi.org/10.1002/zamm.201200179.

[7] I. Elishakoff. Probabilistic resolution of the twentieth century conundrum in elastic stability. *Thin-Walled Structures* 59 (2012), 35–57. DOI: https://doi.org/10.1016/j.tws.2012.04.002.

[8] H. Wagner et al. Robust design of imperfection sensitive thin-walled shells under axial compression, bending or external pressure. *International Journal of Mechanical Sciences* 156 (2019), 205–220. DOI: https://doi.org/10.1016/j.ijmecsci.2019.02.047.

[9] Y. Vetyukov et al. Mixed Eulerian—Lagrangian description in materials processing: deformation of a metal sheet in a rolling mill. *International Journal for Numerical Methods in Engineering* 109.10 (2017), 1371–1390. DOI: https://doi.org/10.1002/nme.5314.

[10] T. Firbank. Mechanics of the belt drive. *International Journal of Mechanical Sciences* 12.12 (1970), 1053–1063. DOI: https://doi.org/10.1016/0020-7403(70)90032-9.

[11] T. Morimoto and H. Iizuka. Rolling contact between a rubber ring and rigid cylinders: Mechanics of rubber belts. *International Journal of Mechanical Sciences* 54.1 (2012), 234–240. DOI: https://doi.org/10.1016/j.ijmecsci.2011.11.001.

[12] D. G. Alciatore and A. E. Traver. Multipulley Belt Drive Mechanics: Creep Theory vs Shear Theory. *Journal of Mechanical Design* 117.4 (1995), 506–511. DOI: 10.1115/1.2826711.

[13] H. Zhu, W. Zhu and W. Fan. Dynamic modeling, simulation and experiment of power transmission belt drives: A systematic review. *Journal of Sound and Vibration* 491 (2021), 115759. DOI: https://doi.org/10.1016/j.jsv.2020.115759.

[14] Y. Vetyukov et al. Flexible belt hanging on two pulleys: Contact problem at non-material kinematic description. *International Journal of Solids and Structures* 168 (2019), 183–193. DOI: https://doi.org/10.1016/j.ijsolstr.2019.03.034.

[15] C. Schmidrathner and Y. Vetyukov. Non-material Finite Elements for Spatial Deformations of Belts. *Contributions to Advanced Dynamics and Continuum Mechanics*. Springer International Publishing, 2019, 227–242. DOI: 10.1007/978-3-030-21251-3_13.

[16] J. Scheidl. Motion of a friction belt drive at mixed kinematic description. *International Journal of Solids and Structures* 200-201 (2020), 158–169. DOI: https://doi.org/10.1016/j.ijsolstr.2020.05.001.

[17] J. Scheidl and Y. Vetyukov. Steady motion of a slack belt drive: dynamics of a beam in frictional contact with rotating pulleys. *Journal of Applied Mechanics* (2020), 1–42. DOI: 10.1115/1.4048317.

[18] K. Dufva et al. Nonlinear dynamics of three-dimensional belt drives using the finite-element method. *Nonlinear Dynamics* 48.4 (2007), 449–466. DOI: 10.1007/s11071-006-9098-9.

[19] E. Oborin, Y. Vetyukov and I. Steinbrecher. Eulerian description of non-stationary motion of an idealized belt-pulley system with dry friction. *International Journal of Solids and Structures* 147 (2018), 40–51. DOI: https://doi.org/10.1016/j.ijsolstr.2018.04.007.

[20] K. Davey and M. Ward. A practical method for finite element ring rolling simulation using the ALE flow formulation. *International Journal of Mechanical Sciences* 44.1 (2002), 165–190. DOI: https://doi.org/10.1016/S0020-7403(01)00080-7.

[21] H. Askes, E. Kuhl and P. Steinmann. An ALE formulation based on spatial and material settings of continuum mechanics. Part 2: Classification and applications. *Computer Methods in Applied Mechanics and Engineering* 193.39 (2004), 4223–4245. DOI: https://doi.org/10.1016/j.cma.2003.09.031.

[22] L. Foucard et al. A coupled Eulerian–Lagrangian extended finite element formulation for simulating large deformations in hyperelastic media with moving free boundaries. *Computer Methods in Applied Mechanics and Engineering* 283 (2015), 280–302. DOI: https://doi.org/10.1016/j.cma.2014.09.016.

[23] J.-W. Liu et al. An efficient multibody dynamic model of three-dimensional meshing contacts in helical gear-shaft system and its solution. *Mechanism and Machine Theory* 142 (2019), 103607. DOI: https://doi.org/10.1016/j.mechmachtheory.2019.103607.

[24] H. Zhang et al. An efficient multibody dynamic model of arresting cable systems based on ALE formulation. *Mechanism and Machine Theory* 151 (2020), 103892. DOI: https://doi.org/10.1016/j.mechmachtheory.2020.103892.

[25] V. Longva and S. Sævik. A Lagrangian–Eulerian formulation for reeling analysis of history-dependent multilayered beams. *Computers & Structures* 146 (2015), 44–58. DOI: https://doi.org/10.1016/j.compstruc.2014.09.002.

[26] V. Longva and S. Sævik. On prediction of torque in flexible pipe reeling operations using a Lagrangian–Eulerian FE framework. *Marine Structures* 46 (2016), 229–254. DOI: https://doi.org/10.1016/j.marstruc.2016.01.004.

[27] H. Irschik and H. J. Holl. The equations of Lagrange written for a non-material volume. *Acta Mechanica* 153.3 (2002), 231–248. DOI: 10.1007/BF01177454.

[28] A. Steinboeck, M. Saxinger and A. Kugi. Hamilton's Principle for Material and Nonmaterial Control Volumes Using Lagrangian and Eulerian Description of Motion. *Applied Mechanics Reviews* 71.1 (2019), 010802. DOI: https://doi.org/10.1115/1.4042434.

[29] K.-D. Chen et al. Equivalence of Lagrange's equations for non-material volume and the principle of virtual work in ALE formulation. *Acta Mechanica* 231.3 (2020), 1141–1157. DOI: 10.1007/s00707-019-02576-8.

[30] D. Hong and G. Ren. A modeling of sliding joint on one-dimensional flexible medium. *Multibody System Dynamics* 26.1 (2011), 91–106. DOI: 10.1007/s11044-010-9242-7.

[31] P. Hyldahl, A. Mikkola and O. Balling. A thin plate element based on the combined arbitrary Lagrange–Euler and absolute nodal coordinate formulations. *Proceedings of the Institution of Mechanical Engineers, Part K: Journal of Multi-body Dynamics* 227.3 (2013), 211–219. DOI: 10.1177/1464419313480351.

[32] A. Pechstein and J. Gerstmayr. A Lagrange–Eulerian formulation of an axially moving beam based on the absolute nodal coordinate formulation. *Multibody System Dynamics* 30.3 (2013), 343–358. DOI: 10.1007/s11044-013-9350-2.

[33] J. L. Escalona, G. Orzechowski and A. M. Mikkola. Flexible multibody modeling of reeving systems including transverse vibrations. *Multibody System Dynamics* 44.2 (2018), 107–133. DOI: 10.1007/s11044-018-9619-6.

[34] J.-P. Liu, Z.-B. Cheng and G.-X. Ren. An Arbitrary Lagrangian–Eulerian formulation of a geometrically exact Timoshenko beam running through a tube. *Acta Mechanica* 229.8 (2018), 3161–3188. DOI: 10.1007/s00707-018-2161-z.

[35] A. Huynen, E. Detournay and V. Denoël. Eulerian formulation of elastic rods. *Proceedings of the Royal Society A: Mathematical, Physical and Engineering Sciences* 472.2190 (2016), 20150547. DOI: 10.1098/rspa.2015.0547.

[36] Y. Vetyukov. Non-material finite element modelling of large vibrations of axially moving strings and beams. *Journal of Sound and Vibration* 414 (2018), 299–317. DOI: https://doi.org/10.1016/j.jsv.2017.11.010.

[37] J. Synka and A. Kainz. A novel mixed Eulerian–Lagrangian finite-element method for steady-state hot rolling processes. *International Journal of Mechanical Sciences* 45.12 (2003), 2043–2060. DOI: https://doi.org/10.1016/j.ijmecsci.2003.12.008.

[38] K. Grundl et al. ALE beam using reference dynamics. *Multibody System Dynamics* 46.2 (2019), 127–146. DOI: 10.1007/s11044-019-09671-7.

[39] A. Humer, I. Steinbrecher and L. Vu-Quoc. General sliding-beam formulation: A non-material description for analysis of sliding structures and axially moving beams. *Journal of Sound and Vibration* 480 (2020), 115341. DOI: https://doi.org/10.1016/j.jsv.2020.115341.

[40] Y. Vetyukov et al. Transient modelling of flexible belt drive dynamics using the equations of a deformable string with discontinuities. *Mathematical and Computer Modelling of Dynamical Systems* 23.1 (2017), 40–54. DOI: 10.1080/13873954.2016.1232281.

[41] Y. Vetyukov, P. G. Gruber and M. Krommer. Nonlinear model of an axially moving plate in a mixed Eulerian–Lagrangian framework. *Acta Mechanica* 227.10 (2016), 2831–2842. DOI: 10.1007/s00707-016-1651-0.

[42] P. Naghdi and M. Rubin. On the significance of normal cross-sectional extension in beam theory with application to contact problems. *International Journal of Solids and Structures* 25.3 (1989), 249–265. DOI: https://doi.org/10.1016/0020-7683(89)90047-4.

[43] L. Nikitin et al. On the frictional behaviour of thermally loaded beams resting on a plane. *International Journal of Mechanical Sciences* 38.11 (1996), 1219–1229. DOI: https://doi.org/10.1016/0020-7403(96)00009-4.

[44] A. Gasmi et al. The effect of transverse normal strain in contact of an orthotropic beam pressed against a circular surface. *International Journal of Solids and Structures* 49.18 (2012), 2604–2616. DOI: https://doi.org/10.1016/j.ijsolstr.2012.05.022.

[45] A. K. Belyaev et al. Contact of two equal rigid pulleys with a belt modelled as Cosserat nonlinear elastic rod. *Acta Mechanica* 228.12 (2017), 4425–4434. DOI: 10.1007/s00707-017-1942-0.

[46] E. Oborin and Y. Vetyukov. Steady state motion of a shear deformable beam in contact with a traveling surface. *Acta Mechanica* 230.11 (2019), 4021–4033. DOI: 10.1007/s00707-019-02476-x.

[47] E. Oborin. Belt–pulley interaction: role of the action line of friction forces. *Acta Mechanica* 231.9 (2020), 3979–3987. DOI: 10.1007/s00707-020-02724-5.

[48] V. Eliseev. Mechanics of deformable solid bodies. St. Petersburg: St. Petersburg State Polytechnical University Publishing House, 2006.

[49] V. V. Eliseev and Y. M. Vetyukov. Finite deformation of thin shells in the context of analytical mechanics of material surfaces. *Acta Mechanica* 209.1 (2009), 43–57. DOI: 10.1007/s00707-009-0154-7.

[50] Y. Vetyukov. Nonlinear Mechanics of Thin-Walled Structures. Asymptotics, Direct Approach and Numerical Analysis. Foundations of Engineering Mechanics. Vienna: Springer, 2014, 272.

[51] V. Berdichevskii. Variational-asymptotic method of constructing a theory of shells: PMM vol. 43, no.4, 1979, pp. 664–687. *Journal of Applied Mathematics and Mechanics* 43.4 (1979), 711–736. DOI: https://doi.org/10.1016/0021-8928(79)90157-6.

[52] W. Koiter. On the foundations of the linear theory of thin elastic shells. *Proc. Kon. Ned. Akad. Wetensch.* B73 (1970), 169–195.

[53] V. Eliseev and Y. Vetyukov. Theory of shells as a product of analytical technologies in elastic body mechanics. *Shell Structures: Theory and Applications - Proceedings of the 10th SSTA 2013 Conference* 3 (2014), 81–84. DOI: 10.1201/b15684-18.

[54] E. Berger. Friction modeling for dynamic system simulation. *Applied Mechanics Reviews* 55.6 (2002), 535–577. DOI: 10.1115/1.1501080.

[55] V. Yastrebov. Numerical Methods in Contact Mechanics. John Wiley & Sons, Ltd, 2013, 392. DOI: 10.1002/9781118647974.

[56] E. Pennestrì et al. Review and comparison of dry friction force models. *Nonlinear Dynamics* 83.4 (2016), 1785–1801. DOI: 10.1007/s11071-015-2485-3.

[57] R. A. Sauer, R. Ghaffari and A. Gupta. The multiplicative deformation split for shells with application to growth, chemical swelling, thermoelasticity, viscoelasticity and elastoplasticity. *International Journal of Solids and Structures* 174-175 (2019), 53–68. DOI: https://doi.org/10.1016/j.ijsolstr.2019.06.002.

[58] E. Hansy-Staudigl and M. Krommer. Electrostrictive polymer plates as electro-elastic material surfaces: Modeling, analysis, and simulation. *Journal of Intelligent Material Systems and Structures* 32.3 (2021), 296–316. DOI: 10.1177/1045389X20935640.

[59] V. Ivannikov, C. Tiago and P. Pimenta. TUBA finite elements: Application to the solution of a nonlinear Kirchhoff-Love shell theory. *Shell Structures: Theory and Applications - Proceedings of the 10th SSTA 2013 Conference* 3 (2014), 97–100.

[60] M. Ambati, J. Kiendl and L. De Lorenzis. Isogeometric Kirchhoff–Love shell formulation for elasto-plasticity. *Computer Methods in Applied Mechanics and Engineering* 340 (2018), 320–339. DOI: https://doi.org/10.1016/j.cma.2018.05.023.

[61] G. Radenković, A. Borković and B. Marussig. Nonlinear static isogeometric analysis of arbitrarily curved Kirchhoff-Love shells. *International Journal of Mechanical Sciences* 192 (2021), 106143. DOI: https://doi.org/10.1016/j.ijmecsci.2020.106143.

[62] F. Bogner, R. Fox and L. Schmit. The generation of interelement compatible stiffness and mass matrices by the use of interpolation formulae. *Proc. 1st Conf. Matrix Methods in Structural Mechanics*. Vol. AFFDL-TR-66-80. Wright Patterson Air force Base, Ohio, 1966, 397–443.

[63] O. Zienkiewicz, R. Taylor and J. Zhu. Chapter 3 - Weak Forms and Finite Element Approximation: 1-D Problems. *The Finite Element Method: its Basis and Fundamentals*. Ed. by O. Zienkiewicz, R. Taylor and J. Zhu. Seventh Edition. Oxford: Butterworth-Heinemann, 2013, 47–92. DOI: https://doi.org/10.1016/B978-1-85617-633-0.00003-4.

[64] F. Frendo and F. Bucchi. "Brush model" for the analysis of flat belt transmissions in steady-state conditions. *Mechanism and Machine Theory* 143 (2020), 103653. DOI: https://doi.org/10.1016/j.mechmachtheory.2019.103653.

[65] K.-J. Bathe, A. Iosilevich and D. Chapelle. An evaluation of the MITC shell elements. *Computers & Structures* 75.1 (2000), 1–30. DOI: https://doi.org/10.1016/S0045-7949(99)00214-X.

Jakob Scheidl

Curriculum Vitae

Contact

3254 Bergland, Austria
jakob.scheidl@tuwien.ac.at

Personal profile

DOB: 26 September 1991
Military Service: 2010

Languages

German, English

Computer literacy

Math: Mathematica, Matlab
Typesetting: LaTeX, TikZ, pgfplots, Office
Programming: F#
FEM: Abaqus
CAD: Catia

Expertise

Structural mechanics, Finite Element Method, Analytical Mechanics, Belt drive mechanics, Contact of Solids, Metal plasticity, Stability of Structures

Education

AHS Wieselburg
High school 2002-2010

TU Wien
Bachelor Program Mechanical Engineering 2011–2016
Thesis: Limiting conditions for the mechanical Autofrettage of a borehole

TU Wien
Master Program Mechanical Engineering 2017–2018
Thesis: Torsional-flexural buckling of a circular rod with a thin-walled open cross section

TU Wien
Doctoral Program Technical Sciences 2018–2021
Thesis: Mixed kinematic modelling and simulation of slack belt drives using structural theories of rods and shells

Experience

TU Wien, Institute of Mechanics and Mechatronics
Research Assistant 2018–2021
Research Group: Mechanics of Solids
Research in the framework of the industrial cooperation project *LaLaBand* funded by the Austrian Research Promotion Agency FFG, grant number 861493.

TU Wien, Institute of Mechanics and Mechatronics
Tutor 2016–2017
Courses on machine dynamics and solid mechanics

Linz Center of Mechatronics (LCM)
Internship 2010
Design of a test rig for hydraulic valves